Comparison of the Corrosion Resistance of New and Innovative Prestressing Strand Types used in the Post Tensioning of Bridges

by

Sean Mac Lean, B.S.A.R.E.

Thesis

Presented to the Faculty of the Graduate School of

The University of Texas at Austin

in Partial Fulfillment

of the Requirements

for the Degree of

Master of Science in Engineering

The University of Texas at Austin

May 2008

Comparison of the Corrosion Resistance of New and Innovative Prestressing Strand Types used in the Post Tensioning of Bridges

Approved by
Supervising Committee:

John E. Breen

Harovel Wheat

Acknowledgements

In my four years as an undergraduate at The University of Texas at Austin I never thought of pursuing a Master's degree. However I am very thankful to all those who have made it possible for their support, it was definitely a worthwhile experience. Most importantly I would like to thank Dr. John Breen for his guidance and direction in undertaking this task. Without the generous support of the Texas Department of Transportation and the Federal Highway Administration however this project would not be possible. So my thanks go out to you.

Special thanks go to Dr. Sharon Wood and the entire civil engineering faculty, without their excellent teaching and inspiration none of this would have been possible. Dr. Andrea Schokker was by far the most influential person in my research and for that I am very thankful; she was there every step of the way for guidance and her assistance will never be forgotten. I will also like to thank Dr. Harovel Wheat and Alex Pacheco for their guidance with my research.

No project can be successful without a supporting staff. I was privileged to have worked with many hard working undergraduate and graduate students. Most importantly were those that worked directly with me on my project. Greg Turco, Ryan Kalinas, Erin O'Malley, Curtis Anderson, Zach Webb, Karl Kleuver and Katherine Abdou I wish you'll well and I am very thankful to have had the opportunity to work alongside you'll. I would also like to thank the administrative staff at FSEL including Blake Stasney, Dennis Fillip, Eric Schell, Mike Wason, Greg Harris, Barbara Howard, Ella Schwartz, and Cari Billingsley for their dedicated support.

Last but by far not least my family, my parents and especially my grandmother, thank you for pushing me to achieve my goals and thank you for your continued support, it is very much appreciated.

Comparison of the Corrosion Resistance of New and Innovative Prestressing Strand Types used in the Post Tensioning of Bridges

Sean Mac Lean, M.S.E.

The University of Texas at Austin, 2008

SUPERVISOR: John Breen

Project 4562 was launched with support from the Texas Department of Transportation and the Federal Highway Administration. The project was designed to test the relative corrosion resistance of various post-tensioned systems. These systems have utilized new and innovative strand types not commonly used in current post-tensioning projects. The project consists of various parts including large beam exposures. These large beam specimens are currently being exposed to a salt solution cycle at the Phil M. Ferguson Structural Engineering Laboratory at the University of Texas at Austin. From a previous project that was similar in scale it was noticed that there was a need to know the corrosive properties before the autopsy of the large specimens. The grouts and grouting techniques had previously been tested by various researchers. Therefore it was important to establish the corrosive properties of the strands used in the post-tensioning of the large beam specimens. The goals of this research were to:

i. Determine the mechanical properties including modulus information of the different strand types that were used in the large beam specimens. These mechanical properties were not determined before the strands were placed in the beam specimens.

ii. Establish the corrosive properties of the different strand and grout interactions. This included establishing an appropriate testing technique to compare times to corrosion.

These objectives were achieved in two stages. The mechanical properties of the strands were determined first. A test setup was designed for easy testing. This setup was used for all the mechanical testing done on the strand specimens. The corrosive properties of the different strand and grout interactions were then established. Different electrochemical testing techniques were employed to attain the corrosive properties. Most importantly was the use of the linear polarization resistance testing technique to compare the times to corrosion for each strand specimen.

Table of Contents

List of Tables

List of Figures

CHAPTER 1
Introduction

1.1 BACKGROUND

The wide use of prestressing systems in today's bridges has spawned interest in new and improved methods of prestressing. New materials and combinations of these materials are being used to prevent failures due to corrosion. However, the high strength materials used in today's prestressed systems can still be highly vulnerable to corrosion especially in high chloride environments. This problem occurs rarely in pretensioned concrete but has occurred more with post-tensioned systems. In an effort to investigate the effects of corrosion in post-tensioning and methods that can be efficiently used to prevent it, a research project was launched by The Texas Department of Transportation and the Federal Highway Administration[22]. This is an ongoing project that has produced a plethora of important research and has also helped develop new post-tensioning systems and test methods.

The corrosion in post-tensioned bridges is not a rare occurrence. In fact a number of cases have been reported. The problem is that once the tendons are in place, it is extremely difficult to detect problems unless the bridges are regularly monitored. In 2000 a problem with some post-tensioned bridges in Florida was discovered[13]. Substantial corrosion was found on two main bridges in Florida, the Mid-Bay Bridge and the Sunshine Skyway Bridge[13]. Problems were also discovered on 17 of the bridges in Florida[13]. This started a major investigation into the grouting techniques and the grouts used at the time. Major voids in the grout were the main blame for the state of Florida's bridges. In a recent inspection of the Varina-Enon Bridge in Virginia it was noticed that one of the tendons

beneath the deck had completely failed[13]. The area where failure occurred had actually been fixed several years before. In this area there were voids noticed in the existing cement grout. The voids were ultimately filled with high performance grouts. A lot of research has been done to establish techniques for grouting and to develop new grouts to help curb these corrosion problems[12, 16, 18 & 23]. An accelerated corrosion testing technique was developed to test the grouts before use in the field[12, 16, 18 & 23]. This method is currently a standard test acknowledged by the Post-Tensioning Institute.

For any post-tensioning application to work effectively, all the parts must function together. It has been noticed that even if the new grouting techniques are followed it is possible that the internal strands can be exposed to outside corrosive agents most notably chlorides[27]. In post-tensioned systems the grout is placed after the system has been tensioned. Therefore the grout itself is not prestressed. Grout has similar properties to concrete and is not very strong in tension. Once the structure has been put in service the grout can be subjected to tension and this can cause cracks. The ducts that encase the grout may have areas where moisture can penetrate. It is possible that this moisture will get to the strands and cause corrosion to occur. Thus it is important that the strands themselves be capable of avoiding corrosion.

This is also a common problem with suspension bridges. The tendons in many suspension bridges are not grouted to allow for easy removal and inspection of the strands. The strands can be left open to the environment and corrosion is a major problem. Currently British engineers are attempting to repair three of their major suspension bridges[21]. Due to humidity in the main-cables, rust has become a problem. The preferred cure for this problem is to dehumidify the cables to slow down the corrosion. The Japanese have turned to a dry-air injection system as a preventative measure[21]. The problems that are plaguing the current infrastructure

may be avoided if there was a strand with the required strength and also high corrosion resistance.

1.2 OBJECTIVES OF RESEARCH

Project 4562 currently underway at The Ferguson Structural Engineering Laboratory at The University of Texas at Austin was designed to investigate new post-tensioning systems. These include new strand types and also new plastic ducts that were available when the project was started in 2003. Currently all the materials and systems being investigated in this project are being exposed to a high chloride environment in large scale specimens. They are exposed to a wet and dry cycle schedule which includes two weeks of salt water exposure and then two weeks with no water. The beams will go through this schedule for 4-8 years and then will be autopsied (see Ahern 2005).

Project 1405 was very similar to this project although the beams were much larger. Although the autopsy results for project 1405 (see Turco 2007) showed significant corrosion, most of the materials and the procedures used in their construction were outdated when they were eventually autopsied. In an effort to determine how the new post-tensioned systems will perform in their current 4-8 year cycle an Accelerated Corrosion Test was developed to compare the different strand types in the current beams. In this way it may be possible to predict the outcome of the long term exposure testing. Standard tension tests were also done to compare the strengths and mechanical properties of the various strands.

This thesis will document the mechanical properties and the corrosion resistance of these new post-tensioning materials. It will also detail standard test methods for tension and corrosion testing of different strand types.

1.3 MATERIALS TESTED

Only the different strand types were tested in this part of the research project. A brief description and pictures of each strand type are shown below.

1.3.1 Conventional Strand

The conventional strand used for the baseline reference was 7-wire, bare steel, low-relaxation strand. In the tension tests both a 0.5 in. and a 0.6 in. conventional strand were used. For the corrosion testing only the 0.6 in. conventional strand was used. The 0.5 in. conventional strand is shown in Figure 1-1.

Figure 1-1: 0.5 in. conventional strand[1]

1.3.2 Hot Dip Galvanized

The hot dip galvanized strand was supplied by a well known post-tensioner. The conventional strand is dipped in molten zinc which coats the exposed steel. In the hot dip process the strands are not evenly coated and there could be places that contain more zinc than others. The strength of the strands is also reduced due to the heat of the molten zinc. The benefit is that the zinc being more anodic than the steel strand is sacrificed which helps protect the steel strand

beneath from corrosion. The 0.5 in. hot dip galvanized strand is shown in Figure 1-2.

Figure 1-2: 0.5 in. hot dip galvanized strand[1]

1.3.3 Stainless Steel

The stainless steel strand shown in Figure 1-3 was provided by Techalloy Company, Inc. It was originally produced for a bridge project but was replaced by conventional strand and was not used. Stainless steel is known for its corrosion resistance and is used widely in marine applications. There are however different grades of stainless steel and some have better corrosion resistance than others.

Figure 1-3: 0.6 in. stainless steel strand[1]

1.3.4 Copper Clad

The copper clad strands are comprised of individual steel wires encased in copper. The copper is metallurgically bonded to the steel so that the bond between the copper and the steel is very strong which prevents it from separating. However copper is a softer metal and its tensile strength is nowhere near that of steel. Thus the copper reduces the strength of the entire strand. However copper and its alloys have good corrosion resistance. The 0.5 in. copper clad strand is actually 0.438 in. conventional steel strand clad to make the strand 0.5 in. in diameter. The 0.5 in. copper clad strand shown in Figure 1-4 was produced by Copperweld and is not structural strand.

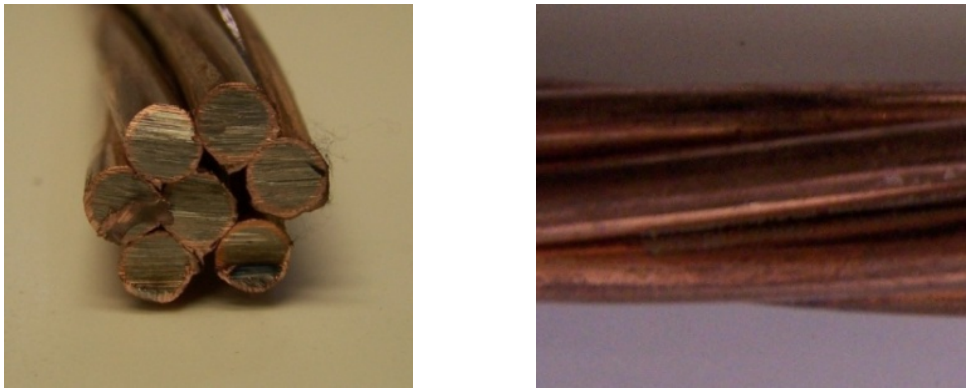

Figure 1-4: 0.5 in. copper clad strand[1]

1.3.5 Stainless Clad

Stainless clad strand provides the user with the strength of conventional steel together with the corrosion protection of stainless steel. Also by having only a thin coating of stainless steel the cost is less than that of a solid stainless steel strand. The cladding process is similar to that of the copper and the steel to stainless steel bond is very strong. The 0.6 in. stainless clad strand shown in Figure 1-5 was supplied by Dywidag Systems International (DSI).

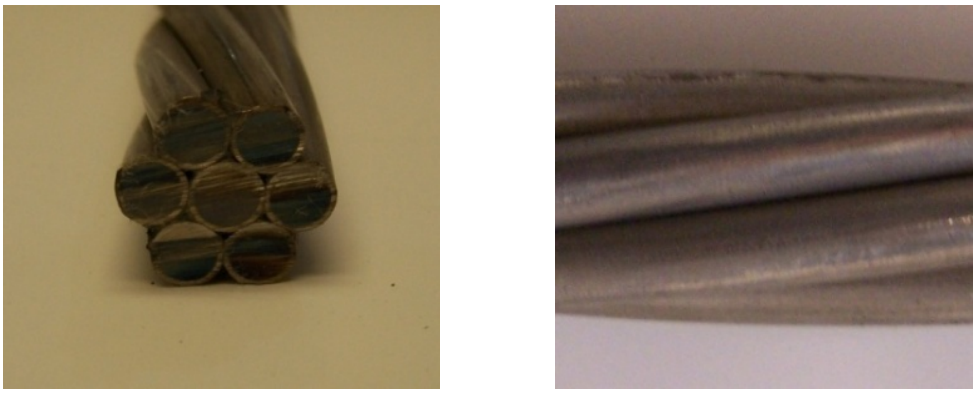

Figure 1-5: 0.6 in. stainless clad strand[1]

1.3.6 Flow- Filled Epoxy Coated

The flow-filled epoxy coated strand is superior to the standard epoxy coated strand. The epoxy gets in the interstitial areas also and prevents moisture from getting into these interstitial areas; thus preventing corrosion from occurring in these areas. The epoxy coating protects the steel strand from corrosion. However if the epoxy is damaged localized corrosion can occur. The epoxy coated strand shown in Figure 1-6 was supplied by Sumiden Wire.

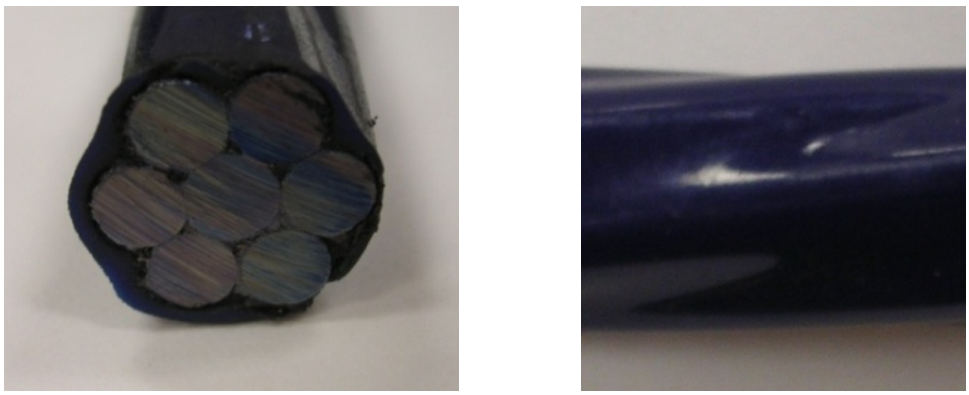

Figure 1-6: 0.5 in. flow-filled epoxy coated strand[1]

1.4 RESEARCH OVERVIEW: CHAPTER OUTLINE

Chapter 2 outlines the tension mechanical testing of the different strand types. The development of an epoxy end grip for use in tension testing of prestressing strands is described in detail. These grips were used to test the strands shown in Section 1.3. The results of the tension tests including the modulus information for each strand are also discussed in this chapter. Conclusions from the testing are shown in the summary.

Chapter 3 gives a general background on corrosion in structural concrete. It highlights some corrosion tests and the theory behind these tests. Most of the tests outlined in this chapter were used to find the corrosive behavior of the strands shown in Section 1.3.

Chapter 4 covers the design and implementation of the accelerated corrosion testing. It describes why the potentiostatic corrosion testing was not a feasible testing technique. The potentiostatic tests were replaced by the linear polarization resistance tests. The accelerated corrosion tests were used to compare the corrosion properties of the strand types shown in Section 1.3. Chapter 4 also shows the equipment used to make the test specimens and also to test them.

The results of the accelerated corrosion tests are shown in Chapter 5. Plots of both the linear polarization resistance tests and the potentiodynamic tests are shown. The results of the linear polarization resistance tests were used to compare the strands.

Chapter 6 lists the findings of all the testing and any recommendations for future testing and development.

CHAPTER 2
Tension Mechanical Testing including Modulus Information

2.1 OVERVIEW

Because the new beam specimens were post-tensioned with new materials many of which had not been previously used in the field, it was important that the mechanical properties be established for each material. The tension tests were therefore done to establish the breaking strength, yield strength and the modulus of elasticity of the various strand types. These properties would be used to first establish if the said materials were able to meet all the specifications required of prestressing strand. Conventional 0.5 in. and 0.6 in. low-relaxation strand were tested along with the other strand types to have a "standard" for comparison. The ASTM A416 (2005) and A370 (2005) guidelines were followed during testing and test preparation. Table 2-1 shows a summary of the testing schedule along with the measured areas of each strand type.

Before the mechanical tests could be performed it was important that a safe and reliable test method be developed that was easily repeatable due to the number of tests that had to be done. This method also needed to be "universal." That is, it must have the capability of testing all the different strand types. In this case the strand diameters ranged from 0.5 in. to 0.6 in. Also, the material type ranged from hot dip galvanized to epoxy coated. The main problem encountered during tension tests of strand is premature failure of one or more of the wires that make up the strand. Generally these failures occur at the grips primarily due to the fact that it is impossible to apply equal force to all 7 wires in the strand while

using conventional grips. Therefore in developing a test method, the primary concern was preventing these end failures.

In addition to the gripping problems there are also high stresses within the strands due to the fact that the strands can get up to over 270 ksi. At these high stresses any small indentations into the individual wires can cause the wires to fracture without warning. The standard grips on the test machines normally have teeth which embed themselves into the material being tested. These teeth help keep the material from slipping and normally help the test to run smoothly. But as mentioned earlier, any indentations in the wires can cause failure. Therefore, it is important to grip the strand indirectly.

Table 2-1: Testing summary showing actual areas of strands

Tension Test Summary			
Type	Nominal Dia. (in)	Area (in^2)	Number of Tests
Conventional	0.5	0.151	3
Galvanize Coated	0.5	0.152	3
Epoxy Coated	0.5	0.153	3
Copper Clad	0.5*	0.144	3
Stainless Clad	0.6*	0.217	3
Conventional	0.6	0.220	3
Stainless Steel	0.6	0.221	3

* includes cladding

All areas were calculated from the measurements of the diameters of the individual wires of each strand (including metallic coating). The copper clad and the stainless clad strand areas shown include the metallic coating. The copper clad strand was actually 0.438 in. diameter conventional strand clad with copper to make it 0.5 in. diameter strand. So the actual area of the steel core was 0.108 in^2. The stainless clad strand was a 0.5 in. diameter conventional strand clad with

stainless steel to make it a 0.6 in. strand. The diameters were measured using a highly precise set of calipers.

2.2 PREVIOUS TESTING TECHNIQUES

Because of the wide use of prestressed concrete in the transportation and other industries it has become important to test the strands used for quality and strength before the strands are used. There have been many techniques employed to prevent the premature failure of the strands during testing. This section will outline these techniques.

All the techniques researched still had end failure problems. There was one technique that involved the use of a FLO-LOC strand grip system that seemed to have had good reviews. Chandu V. Shenoy and Gregory C. Frantz (1991) had done research using this FLO-LOC system manufactured by the Florida Wire and Cable Company. They refined this method by adding standard prestressing chucks to the ends of the strands. The combination worked well because the FLO-LOC sleeves prevented the teeth of the test machine from embedding into the strand and the chucks helped prevent the slipping of the strand. Use of this method still does not guarantee failure outside of the grips however.

Some other methods recommended by H. Kent Preston (1985) include the Sand Grip, the Aluminum Insert, the Tinius Olsen Grip and the PLP Grip. However, the PLP Grip is no longer manufactured. The Tinius Olsen Grip is simply a toothless liner manufactured by the Tinius Olsen Company. The Sand Grip is a little more involved. It consists of aluminum toothless U-grips lined with either 80 grit aluminum oxide and water or sand and oil. This mixture surrounds the strand being tested. The Aluminum Insert is very similar. The strand is surrounded by grease and a mixture of epoxy compound with sand or grit. This is then lined with aluminum angles.

From the literature reviewed none of the previous testing methods seemed to provide a guarantee that the ends would not fail prematurely. Because some of the strand types provided had limited supplies it was important that the test method work without any premature failures. It was therefore decided that a new method be developed.

2.3 SPECIMEN DEVELOPMENT AND PREPARATION

2.3.1 Epoxy End Grips

After reviewing all of the previous testing techniques it was decided that the required time, preparation and cost to conduct testing on a large scale may not be justified. A two-part Type V epoxy had already been provided by Unitex to seal the anchorages on the large beam specimens. The properties of the epoxy made it ideal for use in experiments to form grip ends. The epoxy had a high bonding strength and was not easily crushed. Also by using this epoxy, the forces were transmitted through the greatest surface area of the strands because the epoxy was able to flow not only around the strand but also into the interstitial areas. Initial tension tests showed that the epoxy could withstand the stresses developed in the strands during testing.

2.3.2 Development of Grip Length and Width

Because it is extremely difficult to grip the epoxy itself and stress it to failure, it was not possible to perform tests on the actual epoxy. Instead trial and error was used to find a suitable length and width of grip. As stated earlier, it is extremely difficult to grip the epoxy directly and so there needed to be a medium between the epoxy and the test machine's grips.

Since the test machine that was to be used relied on pressure to grip the ends of the strand, it was important that the shape chosen not be prone to

crushing. Square tubing was considered but was quickly discarded because it was easily crushed when setting up for the tests. Circular tubing was eventually chosen. It was conventional water piping that was then filled with epoxy. The circular tubing was not easily crushed and it had enough surface area for the epoxy bond. A diameter of 1 in. was chosen because it required the least amount of epoxy at the grip ends and there was still room to pour in the epoxy even when using the 0.6 in. diameter strands. Initial tests revealed that the force per length required to severe the bond between the 1 in. piping and the epoxy was far greater than the force per length required to break the bond between the strand and the epoxy. Standard 1 in. metal piping or tubing was therefore chosen as it is also easily available at local hardware stores.

In figuring out a length of grip there was also trial and error used. The ASTM standard for tension testing of wire ropes and strand, ASTM A 931, does not have a requirement for length of strand nor does it have a requirement for grip length. The one requirement however is for the distance between the grips. It says, "The length of test specimen shall not be less than 3 ft, (0.91 m) between sockets for wire ropes up to 1 in." In order to adhere to this one requirement it was decided that the distance between the grips in all specimens be 36 in. The grip lengths were then varied to find a length that was suitable for testing. After a couple tests, a grip length of 18 in. for the 0.5 in. strands and a grip length of 28 in. for the 0.6 in. strands were chosen.

2.3.3 **Specimen Parts Preparation**

For epoxy to bond properly to any material all surfaces must be clean and free of all dust and oil. After cutting the pipes to the lengths needed the inside and outside of the pipes were thoroughly cleaned with acetone and rags. This was an important step since standard water pipes were used. The water pipes have an oily

coating which prevents them from corroding while in storage. Thus, this coating had to be removed using acetone so that the epoxy would easily bond to the pipes.

After a couple tests it was also noticed that although the surfaces of the strands were cleaned with acetone there were still quite a number of failures of the bond between the strand and the epoxy. This was quickly fixed by sand blasting the ends of the strand. The sand blasting removed all foreign elements from the strand surfaces and also created a raw metal surface to which the epoxy easily bonded. The strands were sand blasted with a small abrasive blaster shown in Figure 2-1. The strands were unwrapped at the ends and all the wires were blasted separately to ensure maximum bond.

Figure 2-1: Abrasive Blaster used to sand blast the ends of the strands.

2.3.4 **Specimen Casting**

To make multiple specimens and increase production a setup to cast 3 specimens at a time was built as shown in Figure 2-2. The setup was built using

standard 2 x 4 lumber and was designed to be easily adjustable so that specimens of any length could be cast easily without making drastic adjustments to the setup. The setup also gave the ability to cast both ends of the strand at the same time so they would set at the same time and would be able to be tested sooner. Many of the strands had a natural curvature. The setup held these strands straight so that they would be cast in the same position as they would be tested in.

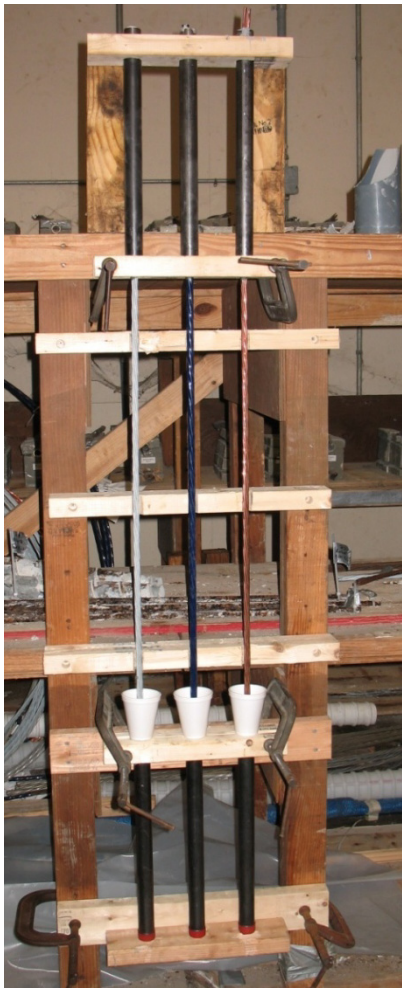

Figure 2-2: Setup used to cast the ends onto the strands; setup has three different strand types that have already been cast.

The ends of the bottom pipes were capped with plastic caps that came with the pipes (see Figure 2-3). Styrofoam cups were then placed on the top of the pipes so that excess epoxy would not spill over onto the setup. The bottom pipes were then clamped in place and the strands inserted. The same caps that were used on the bottom pipes were attached to the bottom of the top pipes. A hole was drilled in each one to allow the strand to pass through into the pipe. To ensure that no epoxy would leak through while casting, a two-part epoxy putty was used to seal the joint between the strand and the caps on the top pipes (see Figure 2-5). This epoxy putty had a 5 minute dry time so there was not much time needed between preparations and pouring of the epoxy. Figure 2-4 shows the top of the setup with the piping clamped in place and strands inserted ready for casting.

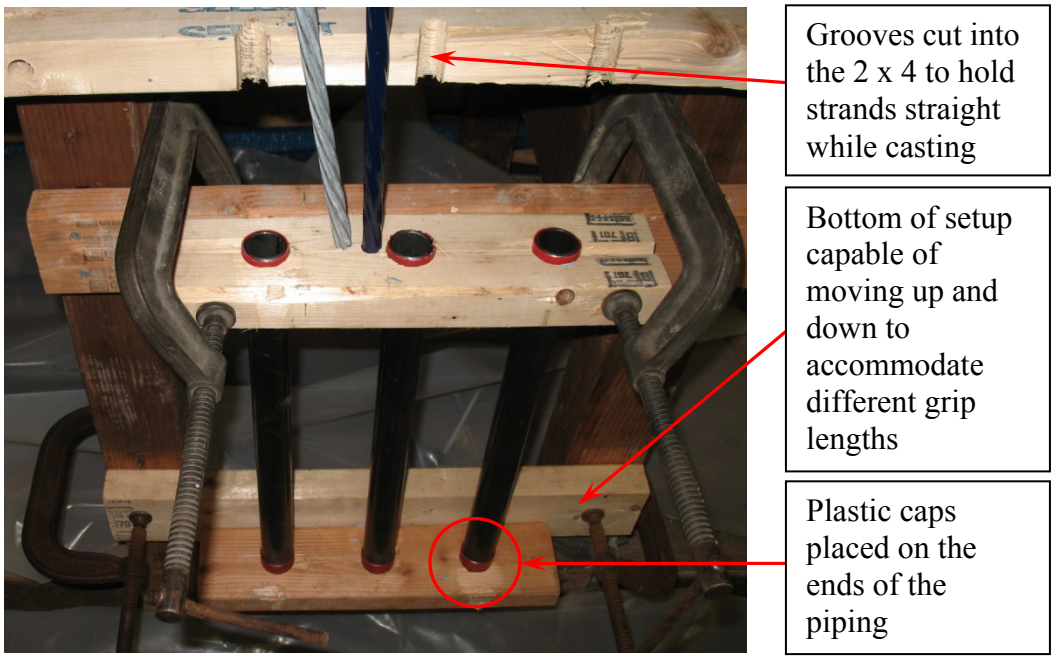

Figure 2-3: Bottom of casting setup before Styrofoam cups and strands have been placed for casting.

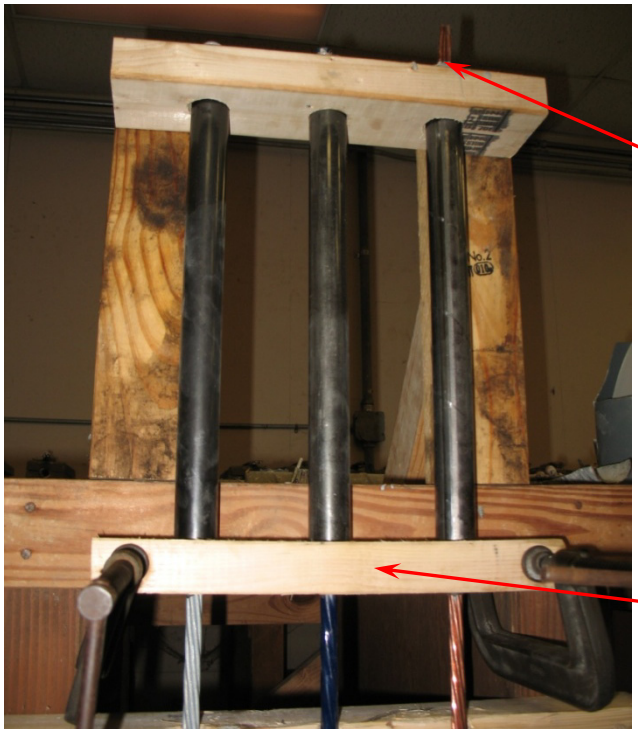

Figure 2-4: Top of casting setup showing piping clamped in place ready for epoxy to be poured from the top.

Figure 2-5: Left: close up of the Styrofoam cups at the top of the bottom piping with the strands inserted ready for casting; Right: close up of the bottom of the top piping showing the epoxy putty which has hardened and is ready for casting.

Once all the pipes were clamped in place and the epoxy putty had dried, the Unitex Pro-Poxy 200 multipurpose bonding adhesive epoxy was mixed. This epoxy requires that you mix 1 part of part A to 1 part of part B and that it be stirred using a high-shear blade with a varying speed drill. Figure 2-6 shows the apparatus used to mix and pour the epoxy. After mixing for the required time the epoxy was poured into the pipes. While pouring, the strands were shaken to get any air bubbles to the surface so that a maximum bond was ensured.

Figure 2-6: 2 part epoxy used to cast ends and mixing apparatus including the high shear blade and variable speed drill.

Although the epoxy only requires 24 hrs to develop its full bonding strength, each specimen was given a minimum of 3 days curing time. However after 1 day, the specimens were removed from the casting setup and cleaned off and prepared for testing. Three days after casting the specimens were all tested.

2.4 SPECIMEN TESTING

2.4.1 Test Setup

With the gripping ends epoxied to the strands the specimens were easily tested in a standard test machine using V-grips. The pipes allowed the test machine's grips to embed into them without damaging the strands. A 600 kip load controlled testing machine manufactured by SATEC Systems Inc., was used to apply the force to the strands as shown in Figure 2-7. The strain was measured using a standard 10 in extensometer manufactured by Epsilon with a travel of 2 in. A 14 in extension also manufactured by Epsilon was attached to the extensometer to make the gage length 24 in as shown in Figure 2-8. The ASTM specification A370 (2005) requires that when determining the elongation of strand used for prestressing concrete a class D extensometer be used and it must have a gage length of no less than 24 in. An extensometer was used instead of measuring cross head movement because during testing there can be slipping of the ends within the grips of the machine and there can also be slipping between the strands and the epoxy.

Figure 2-7: SATEC Systems Inc. 600 kip testing machine with strand specimen in place.

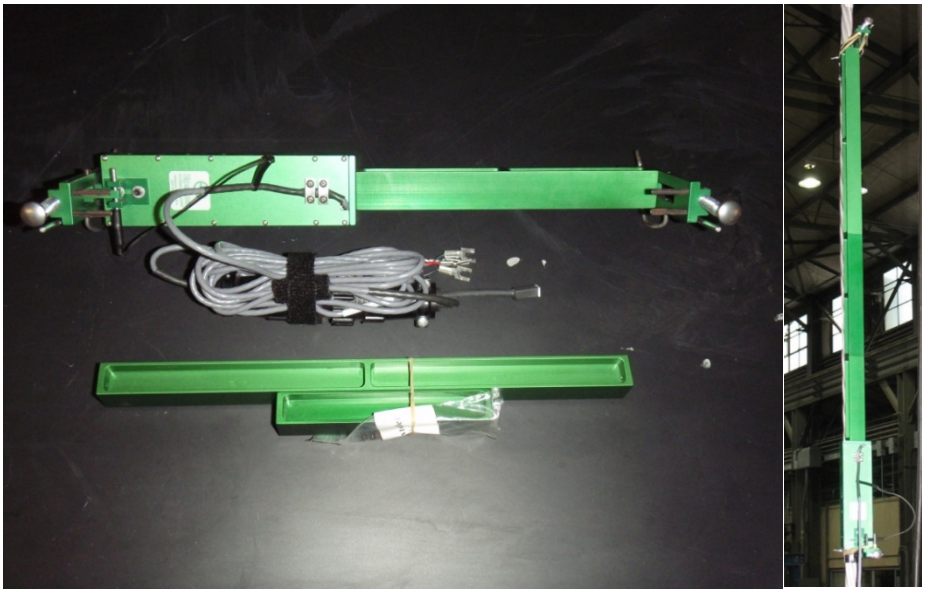

Figure 2-8: 10 in extensometer with the 14 in extension; also shown is the extensometer attached to the strand ready for testing.

2.4.2 Test Procedure

Three specimens per strand type were cast so that three tests per strand type could be performed. The first test was to determine the breaking strength so that a limit for removing the extensometer could be established. This limit was around 90% of the breaking strength. While testing, the load vs. the strain was plotted on the computer in real time and this plot was also taken into consideration before removing the extensometer. This was important so that the extensometer could be left on the specimen for the maximum amount of time.

The strand specimen was placed in the test machine and the grips were secured against the cast ends as shown in Figure 2-9. The specimen was then loaded at an approximate rate of 0.1 kips per second since it was a load controlled machine and not a strain controlled test machine. A small load was applied to the specimen to straighten it out. ASTM A370 (2005) requires that an initial load of 10% of the required minimum breaking strength be applied to the specimen

before the extensometer is placed on the specimen. However as mentioned earlier the first test was done to establish the breaking strength of the strand. This test was therefore done without fixing the extensometer to the specimen. This first specimen was taken from no load to failure load. The failure load and mode of failure were then recorded.

Once the failure load had been established and a benchmark value for removing the extensometer had been determined, the stress-strain tests were ready to be performed. Before the extensometer was fixed to the strand, duct tape was applied to the strand in the areas that the extensometer would be bearing on the strand as shown in Figure 2-10. This was done so that the extensometer would not slip on the strand since the surface of the strand is very smooth. Upon fixing the extensometer to the strand, rubber bands were used to strengthen the connection between the strand and the extensometer.

Figure 2-9: Step 1: Ends secured in the V-grips of the test machine.

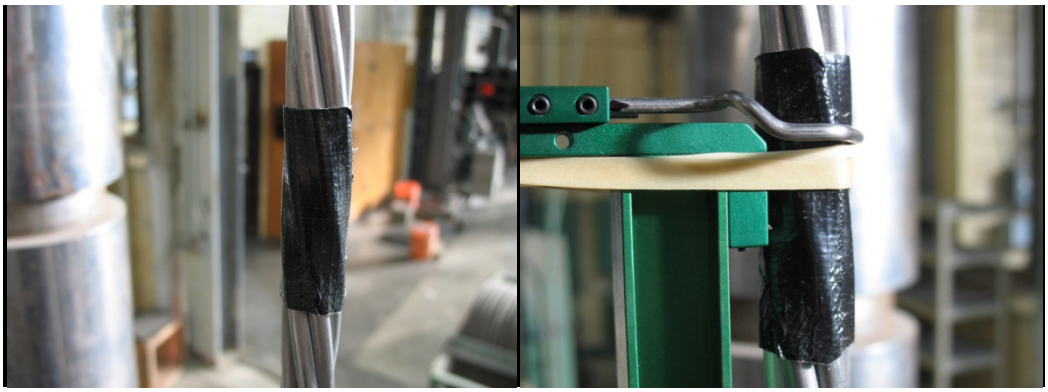

Figure 2-10: Steps 2&3: Duct tape placed on strand in bearing area of extensometer; extensometer has also been placed on strand and secured with rubber bands.

After these initial preparations had been completed, the tests were ready to be performed. All values were zeroed on the computer and the pin holding the extensometer fixed was removed. The load was applied at approximately 0.1 kips per second and the values of the load and elongation were monitored on the computer in real time. Once the load had reached the point where the data was sufficient and it was still safe to be near the specimen without the chance of failure the extensometer was removed. The loading was stopped before removing the extensometer and this process was done as quickly as possible so that not much load in the strand was lost while removing the extensometer. The strand was then loaded to failure and once again the breaking strength and the mode of failure were recorded. A typical failure is shown in Figure 2-11.

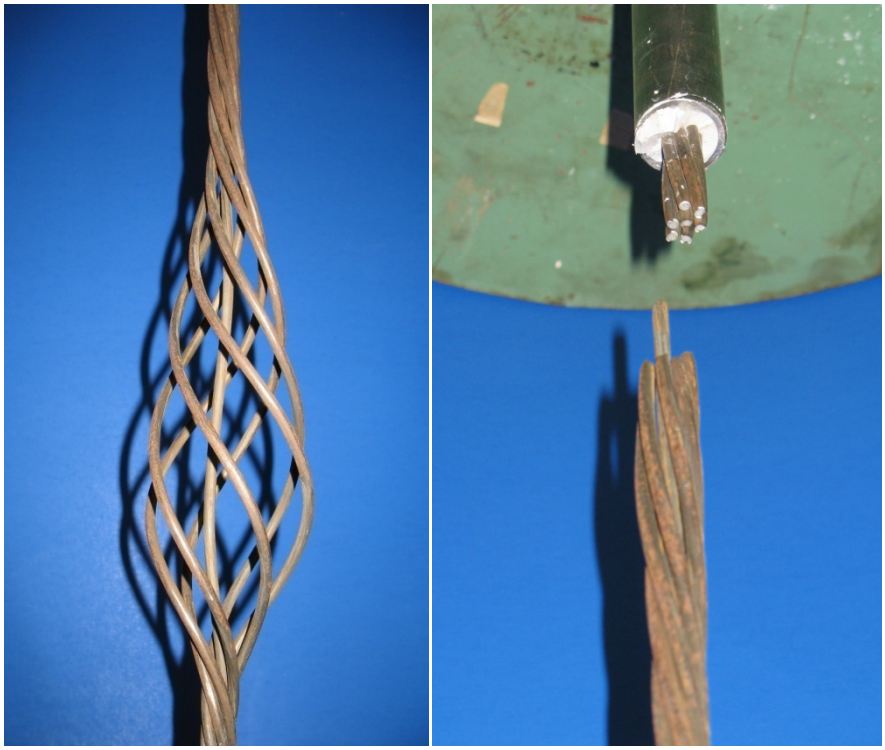

Figure 2-11: Strand specimen after failure had occurred; notice how the outside wires had unwrapped from the interior wire.

2.5 ANALYSIS AND RESULTS

There were 3 tests done per strand type which totaled 21 tests. The first test was to determine the breaking strength of the strand. The second test was to determine the yield strength and the modulus information. Finally, the third test was performed to confirm the results of the second test. This section will outline the results of these 21 tests.

2.5.1 Strand Strength Requirements and Area Modifications

There is no defined specification for some of the strand types tested. The ASTM A 416/A416M specification was thus used to compare all the strands and to provide a specific requirement that each strand must meet. Two of the strands,

(the copper clad and the stainless clad) were comprised of an interior core of conventional steel clad with different metals. The exterior cladding was noticed to be weaker than the core because of the type of metal used. Thus for comparison purposes both the area of the complete strand and the area of the conventional steel core were considered. The total area including the cladding is considered the nominal area and the area of only the steel core is considered the steel area. For the copper clad strand the steel area was found to be 0.108 in^2. Since this area matched that for the strand designation no. 11, this designation was used for the copper clad strand only considering the steel area. The stainless clad strand was a 0.5 in. diameter structural strand clad with stainless steel. Therefore the steel area used for comparison of the stainless clad strand was 0.153 in^2. Table 2-2 shows the yield and breaking strength requirements from ASTM A 416.

Table 2-2: ASTM A 416 requirements

Strand Designation No.	*Nominal Dia. (in)*	*Area (in^2)*	*Minimum Breaking Strength (kip)*	*Yield Strength / Minimum Load at 1% Extension (kip)*	
				Low-Relaxation	Normal-Relaxation
Grade 250					
9	0.375	0.080	20	18.00	17.00
11	0.438	0.108	27	24.30	23.00
13	0.500	0.144	36	32.40	30.60
15	0.600	0.216	54	48.60	45.90
Grade 270					
9	0.375	0.085	23	20.70	19.55
11	0.438	0.115	31	27.90	26.35
13	0.500	0.153	41.3	37.17	35.10
15	0.600	0.217	58.6	52.74	49.80

2.5.2 **Breaking and Yielding Strength**

2.5.2.1 ***Analysis Method***

The load at which the strands failed represents the breaking strength of the strand. The breaking stress can be easily calculated from the load at failure and the area of the strand.

$$\sigma = {}^{P}/_{A}$$

where

σ = the stress in the strand

P = force exerted on the strand by the test machine

A = cross-sectional area of the strand

The yield strength of prestressing strand however is not as well defined. Standard steel reinforcing bars have a well defined yield point and the yield strength can easily be read off of a graph of load vs. strain. The load vs. strain plot of prestressing strand does not have a well defined yield point. Two methods commonly used to find the yield point are the 1% extension method or the 0.2% offset method, both of which are generally accepted. In calculating the yield strength of the strands the 1% extension method was used. This allows for easy comparison to the ASTM A 416 requirements. Figure 2-12 shows how the 1% extension method works in calculating yield strength.

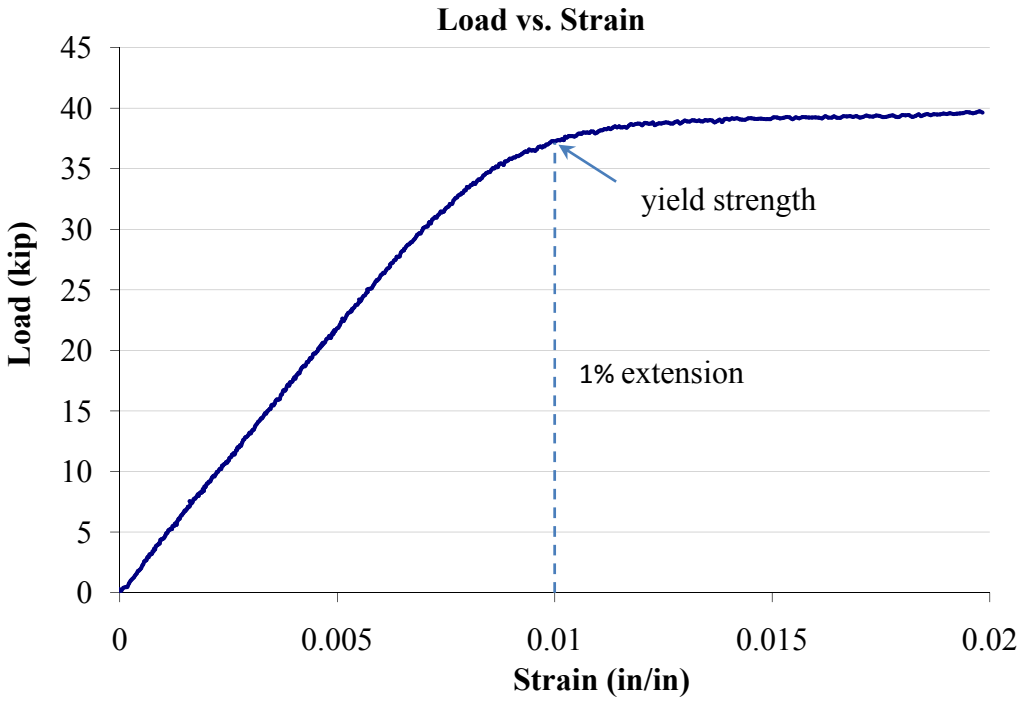

Figure 2-12: Load vs. Strain plot for conventional 0.5 in strand.

2.5.2.2 *Results*

The results presented below are an average of the three tests performed on each strand. The test results were so close that the averages basically represent the values obtained in each test. The breaking strength requirements for prestressing strand are shown in Table 2-2. The values in this table were used as benchmarks for comparing the obtained values. Table 2-3 shows the average tested breaking strength of each strand type.

The stainless steel strand performed very poorly and did not meet either requirement. The copper clad strand was compared using its nominal area and also using the steel area only. Using its nominal area it did not meet the requirements for a 0.5 in. diameter strand. If the cladding is considered non-structural then the 0.438 in. diameter steel core still does not meet the ASTM

requirements. The hot dip galvanized strand although having the area of the Grade 270 conventional steel strand did not meet the strength requirements of the Grade 270 but met the requirements of the Grade 250. This was expected because during the galvanizing process the steel strand is exposed to high temperatures which reduce the strength of the strand. The stainless clad strand did not meet the Grade 270 benchmark either when the stainless cladding was considered part of the structure of the strand. However when the stainless steel was just considered to be a non-structural cladding it met the requirements for the 0.5 in Grade 270 strand. Stainless steel is known to be weaker than conventional steel due to its high carbon content. The stainless cladding on the strand was quite thick and this can reduce its strength.

Table 2-3: Ultimate Strengths

Type	*Nominal Dia. (in)*	*Area (in^2)*	*Breaking Strength (kip)*	*Met Grade 250 requirement*	*Met Grade 270 requirement*
Conventional	0.5	0.153	43.0	Yes	Yes
Epoxy Coated	0.5	0.153	43.7	Yes	Yes
Conventional	0.6	0.217	61.5	Yes	Yes
Hot Dip Galvanized	0.5	0.153	40.9	Yes	No
Stainless Clad (nominal area)	0.6	0.217	57.5	Yes	No
Stainless Clad (steel area)	0.5	0.153	57.5	Yes	Yes
Stainless Steel	0.6	0.217	48.9	No	No
Copper Clad (nominal area)	0.5	0.144	25.9	No	No
Copper Clad (steel area)	0.438	0.108	25.9	No	No

As mentioned earlier the yield strength of prestressing strand is not easily defined and thus it was decided that the 1% extension method be used to establish

the values of the yield strength. Table 2-4 shows the values of the yield strength obtained from the 1% extension method. All of the strand types except for the copper clad and the stainless steel exhibited generally uniform elastic moduli. The copper clad and stainless steel strands seemed to go into the inelastic range almost immediately however. The 1% extension method was still used on both strand types but probably does not accurately represent the yield strength. The table compares the yield strengths obtained to the requirements for low and normal relaxation strands given in ASTM A 416. The results obtained for the yield strengths mirror those obtained for the breaking strength.

Table 2-4: Yield Strengths

Type	*Nominal Dia. (in)*	*Area (in^2)*	*Yield Strength (kip)*	*Met Grade 250 requirement*	*Met Grade 270 requirement*
Conventional	0.5	0.153	37.3	Low & Normal Relaxation	Low & Normal Relaxation
Epoxy Coated	0.5	0.153	37.8	Low & Normal Relaxation	Low & Normal Relaxation
Conventional	0.6	0.217	56.1	Low & Normal Relaxation	Low & Normal Relaxation
Hot Dip Galvanized	0.5	0.153	34.5	Low & Normal Relaxation	Neither
Stainless Clad (nominal area)	0.6	0.217	50.6	Low & Normal Relaxation	Normal Relaxation
Stainless Clad (steel area)	0.5	0.153	50.6	Low & Normal Relaxation	Low & Normal Relaxation
Stainless Steel	0.6	0.217	39.8	Neither	Neither
Copper Clad (nominal area)	0.5	0.144	22.3	Neither	Neither
Copper Clad (steel area)	0.438	0.108	22.3	Neither	Neither

2.5.3 **Elastic and Secant Modulus**

The elastic modulus represents the slope of the elastic part of the curve of the stress-strain graph. For prestressing strand this is generally taken from 10% of the breaking stress to just before the plot starts to curve (see Figure 2-13). The secant modulus is the slope of a line from the origin to any point on the curve (see Figure 2-14). Because prestressing strand is usually stressed to 0.6 P_{Ult}, where P_{Ult} is the maximum breaking strength, the secant modulus was calculated using the origin and this point. For the copper clad and the stainless steel strands there did not seem to be an elastic part to the curve so the elastic modulus was not calculated. Thus the secant modulus for all strand types was calculated to get a comparison.

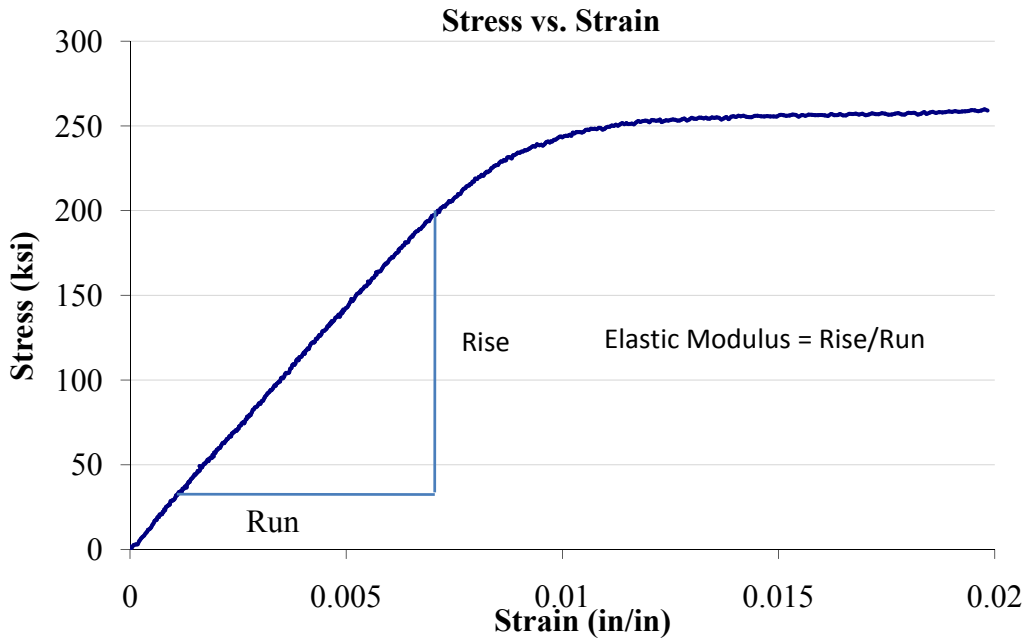

Figure 2-13: Stress vs. Strain plot for conventional 0.5 in strand; plot shows how the elastic modulus is calculated.

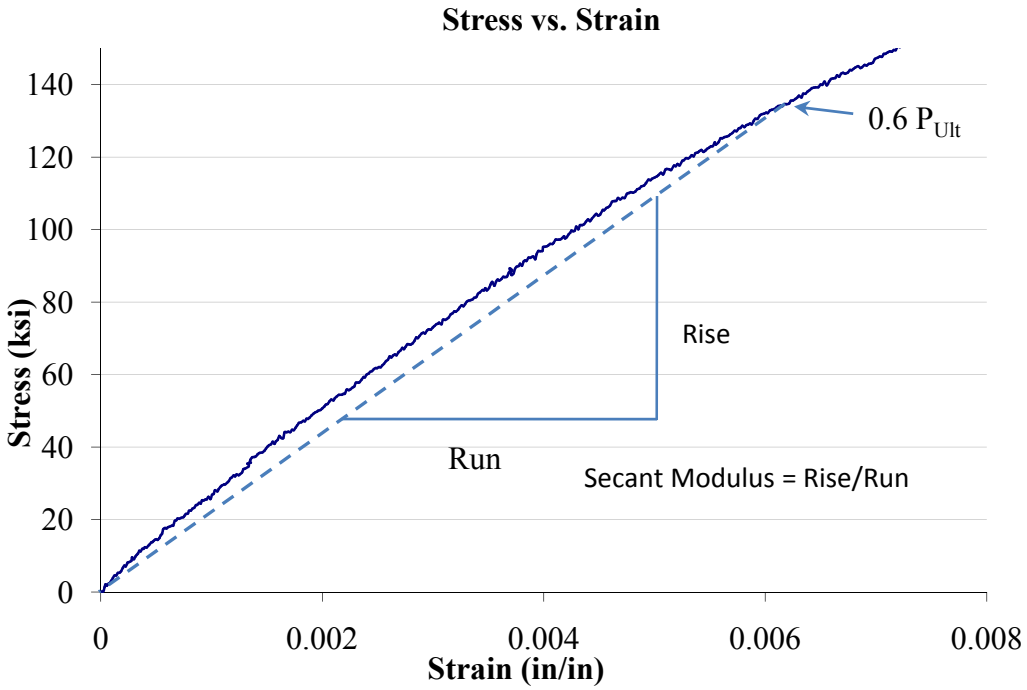

Figure 2-14: Stress vs. Strain plot for stainless steel 0.6 in strand; plot shows how the secant modulus is calculated.

Most of the strands tested had an elastic modulus that was very close to that of steel, 29,000 ksi. The solid stainless steel strand had a secant modulus that was considerably less than that of steel. From its performance in the breaking and yield strength tests it was expected that its modulus would be less. The stainless clad strand had a lower elastic modulus if the nominal area was considered and a much larger modulus if only the steel area was considered. Stainless steel is a metal and thus is part of the structure. To consider it only a cladding would not be accurate. Thus the modulus using the nominal area which is the entire area more accurately estimates the modulus. The same applies to the copper clad strand. However when only the steel core area is used to find the secant modulus for the copper clad strand the secant modulus is very close to that of steel. The elastic and

secant moduli obtained from the tests are shown in Table 2-5. Also included in Figure 2-15 is a stress vs. strain plot of all 7 strand types using their nominal and steel areas for comparison. The great difference between the copper clad and stainless steel strands from the other strands can be seen in the plot in Figure 2-15.

Table 2-5: Elastic and Secant Modulus

Type	*Nominal Dia. (in)*	*Area (in^2)*	*Elastic Modulus (ksi)*	*Secant Modulus (ksi)*
Conventional	0.5	0.153	28664	28609
Epoxy Coated	0.5	0.153	29249	29046
Conventional	0.6	0.217	29396	29378
Hot Dip Galvanized	0.5	0.153	28846	28830
Stainless Clad (nominal area)	0.6	0.217	27148	26725
Stainless Clad (steel area)	0.5	0.153	38505	37904
Stainless Steel	0.6	0.217	-	21116
Copper Clad (nominal area)	0.5	0.144	-	22024
Copper Clad (steel area)	0.438	0.108	-	29365

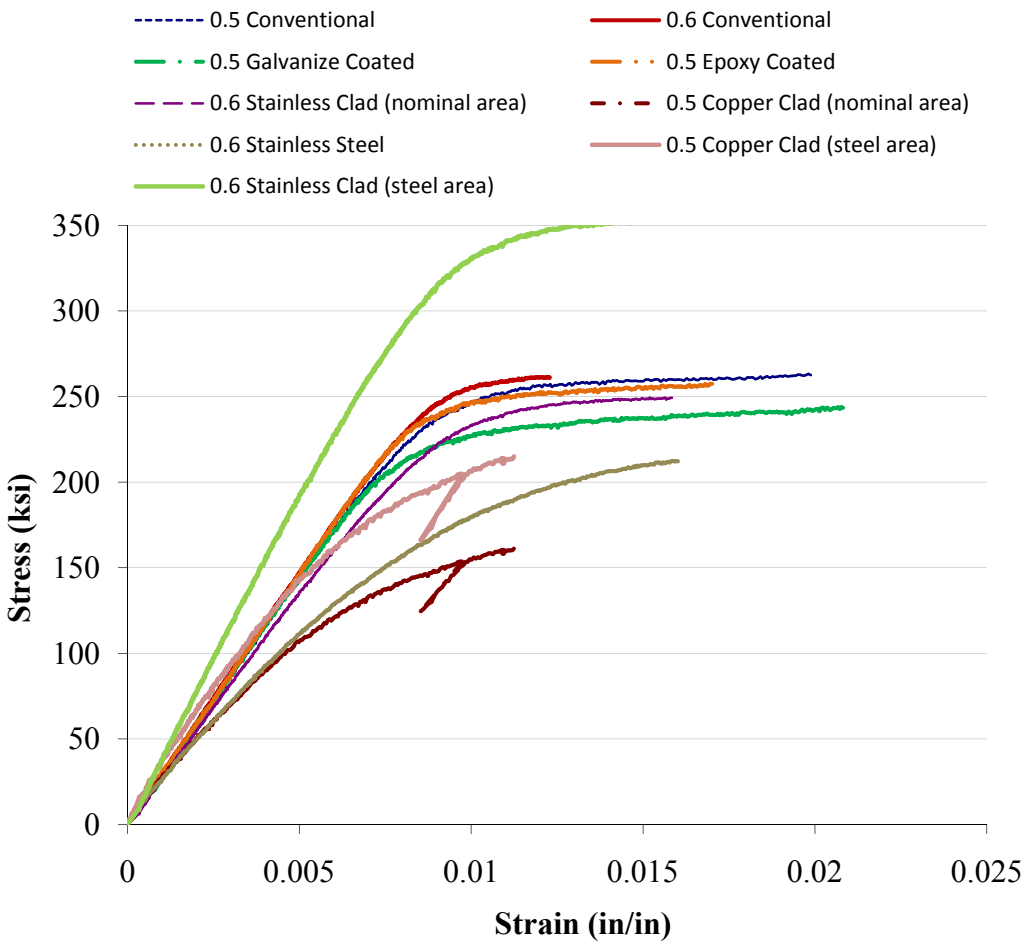

Figure 2-15: Stress vs. Strain plot showing results for each strand type; end of individual plots does not represent failure but only the point at which the extensometer was removed.

2.6 SUMMARY

The main reason for performing the mechanical tests on the various strand types was to determine if the strands being exposed to corrosion testing are suitable for use in the field. Even if all the strand types were to perform well in corrosion testing they can only be cleared for use if their yield and ultimate

strengths and their elastic moduli are up to par. From these initial tests it seems that the stainless steel strand does not meet the requirements for use in the field. The copper clad strand does not meet any of the requirements even if it is considered to be a 0.438 in. diameter conventional strand with a non-structural cladding. These are probably two of the better strands in terms of corrosion resistance and therefore more work needs to be done to develop strands that have their corrosive resistance properties but also can meet all the mechanical requirements.

CHAPTER 3
Corrosion in Structural Concrete

3.1 OVERVIEW

The main objective of project 4562 currently underway at the Phil M. Ferguson Structural Engineering Laboratory in Austin, Texas is to compare the corrosion resistance of different post-tensioned tendon configurations. So although the mechanical properties are very important, it was more important to establish the corrosive aspects of the strand types. This chapter will outline the basic corrosion principles as applied to structural concrete. It will also outline previous testing and the various test methods that have been used to determine corrosion rates and times to corrosion.

3.2 CORROSION IN STRUCTURAL CONCRETE

What makes structural concrete attractive to engineers is the ability to get strength and ductility from a member without the worry that the concrete will deteriorate rapidly. Concrete does not corrode in the way that metals do and so concrete structures can last for longer periods without the maintenance considerations that plague many steel structures. Concrete must be reinforced or prestressed however and this reinforcement or prestressing steel is what becomes susceptible to corrosion. In an ideal environment concrete is a protective barrier for the steel from the elements and other corrosive agents. Over time it has been realized that even very small cracks or voids within the concrete can expose the steel and create problems for structures. Most notably are marine structures and bridges in areas where deicing salts are used. These environments are high in chlorides which accelerate the corrosion process.

Prestressing strands are especially susceptible to corrosion in these environments. The high strength small diameter wires making up the strands become more susceptible to corrosion. Together with that they have high stresses within them at all times so that loss of area due to corrosion can easily bring on failure. In post-tensioned systems the entire system (strand, grout and duct) must function together to assure serviceability. A lot of work has been done with grouts to perfect the actual grout used and also the grouting technique[12, 16, 18, 23]. The grout is a very important part of the system since it helps protect the strands. However it has been learned that in many situations after the grout has dried and the structure has been put into service the grout can crack and allow corrosive agents to attack the strands[22]. The same phenomenon happens with standard reinforced concrete and research has been done into coating and protecting the actual reinforcement.

The next few chapters of this thesis will examine the corrosive properties of the various strand types that were available for testing in 2003 when this program was undertaken. The corrosive behaviors of each strand type will be investigated. These behaviors will be used to compare the strand types side by side. The objective was not to compare grouts. It was to compare how the interaction between each strand type and a single grout in a corrosive environment affects the time until corrosion has initiated.

3.2.1 Corrosion of Metals

Corrosion of metals is a destructive process. Metallic corrosion usually occurs on the surface between the metal and the electrolyte solution. The exposed surface breaks down into undesirable elements. In some cases the corrosion can actually help to protect the surface. As the metal oxidizes it forms an oxide layer that is more stable than the original metal surface. The metal surface becomes

more stable, passivates and the corrosion process slows down almost to a halt[15]. In certain environments however, such as those high in chlorides, once corrosion has initiated it will continue until the metal has completely broken down.

Corrosion in metals is mostly due to electrochemical reactions. These can be divided into anodic and cathodic reactions; the anodic reaction being an oxidation reaction and the cathodic reaction being a reduction reaction. Equations 3-1 and 3-2 show the common anodic and cathodic reactions for iron in a moist and oxygenated environment[15].

$Fe \rightarrow Fe^{2+} + 2e^-$ (anodic/oxidation reaction) ***Equation 3-1***

$2H_2O + O_2 + 4e^- \rightarrow 4OH^-$ (cathodic/reduction reaction) ***Equation 3-2***

The reactions above show what may happen to conventional prestressing steel when exposed to freshly poured concrete or grout. Note that the reaction is dependent on both water and oxygen. Thus, if there is a break in the protective surface (grout) the reactions will speed up if there is also a supply of moisture and air. In the anodic reaction the metal being oxidized loses electrons. These electrons flow from the area where the anodic reaction is taking place to where the cathodic reaction is taking place. These two areas may be two different metals or can be two different spots on the same metal with slightly different properties. These electrons then combine with water and oxygen to produce hydroxyl ions. A combination of these hydroxyl ions and the iron ions produces what we know as rust, $Fe(OH)_3$. The reactions and elements involved are somewhat different for different metals but in general they follow the same electrochemical process. Figure 3-1 shows a simplified diagram of the corrosion process.

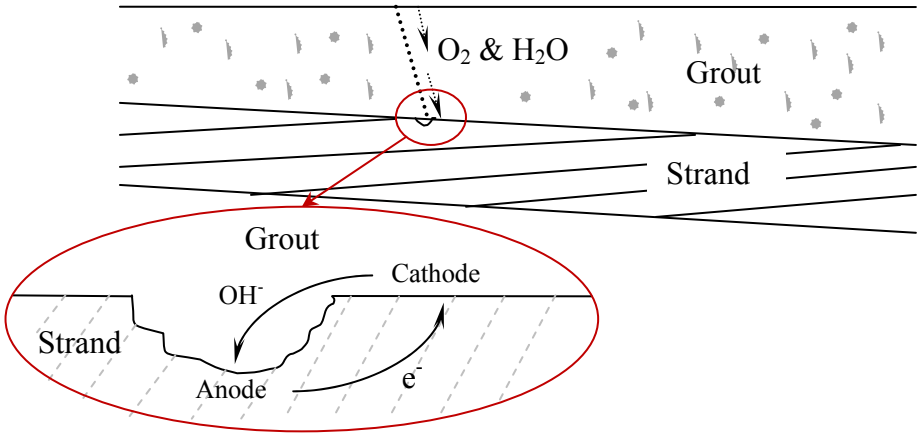

Figure 3-1: Corrosion Process of Conventional Strand Encased in Grout

3.2.2 Passivity of Metals

Many metals have active, passive and transpassive ranges. The range in which the metal falls depends on the environment in which the metal is in as well as the potential of the system. The active range is where the metal is most vulnerable and the corrosion rate is the highest. In a passive state the metal forms a protective oxide layer that slows the corrosive process considerably, possibly even stopping it. The transpassive range is the range after the metal has gone through its passive range. This only occurs at high potentials. The properties of concrete increase the possibility that the encased strand will be in a passive state. The concrete or grout encasing the strand has a high pH and high oxygen content which are important for the metal to stay passive. The passive film on the strand is easily broken down by introducing chlorides and lowering the pH in the surrounding concrete (Schokker 1999). If the passive film breaks down in local areas significant metal corrosion can occur in a small area. This is known as pitting. The corrosion rate is very dependent on which range the metal is in as shown in Figure 3-2.

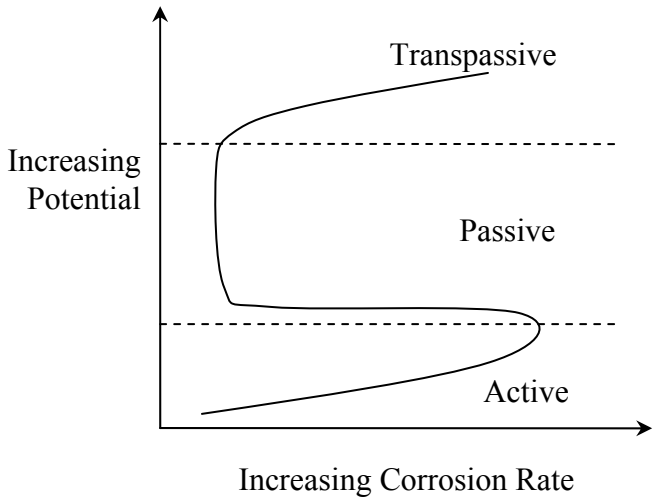

Figure 3-2: General Behavior of Conventional Steel

3.2.3 Half-cell Reactions

The anodic and cathodic reactions occurring are known as half-cell reactions. When combined they make a complete or total electrochemical cell. By separating these half-cell reactions and instrumenting the electrodes on which they occur it is possible to measure the current flow between them. It is important that the oxidation/anodic reactions occur on the strand being tested (working electrode). The counter electrode must therefore be a noble metal which has a higher electromotive force (EMF) potential. The counter electrode chosen was platinum, Pt because it is high on the noble side of the EMF series (see Table 3-1).

Table 3-1: Standard Electromotive Force Potentials (Reduction Potentials)[15]

	Reaction	Standard Potential, e^0 (volts vs. SHE [a])
	$Cl_2 + 2e^- = 2Cl^-$	+1.358
	$O_2 + 4H^+ + 4e^- = 2H_2O$ (pH 0)	+1.229
	$Pt^{2+} + 3e^- = Pt$	+1.118
More	$O_2 + 2H_2O + 4e^- = 4OH^-$ (pH 14)	+0.401
Noble	$Cu^{2+} + 2e^- = Cu$	+0.342
	$2H^+ + 2e^- = H_2$	0.000
	$Ni^{2+} + 2e^- = Ni$	-0.250
	$Fe^{2+} + 2e^- = Fe$	-0.447
	$Cr^{3+} + 3e^- = Cr$	-0.744
	$Zn^{2+} + 2e^- = Zn$	-0.762

[a] Standard Hydrogen Electrode

To measure the half-cell potential or corrosion potential of the working electrode another electrode must be placed in the system. This electrode has a known electromotive force potential and the potential of the working electrode is measured in terms of this electrode. This concept is used to monitor reinforced concrete systems in the field. The Saturated Calomel Electrode (SCE) is normally used as the reference electrode for taking these measurements. A simple system set up is shown in Figure 3-3. Also shown in Table 3-2 are the half-cell potentials of some common reference electrodes.

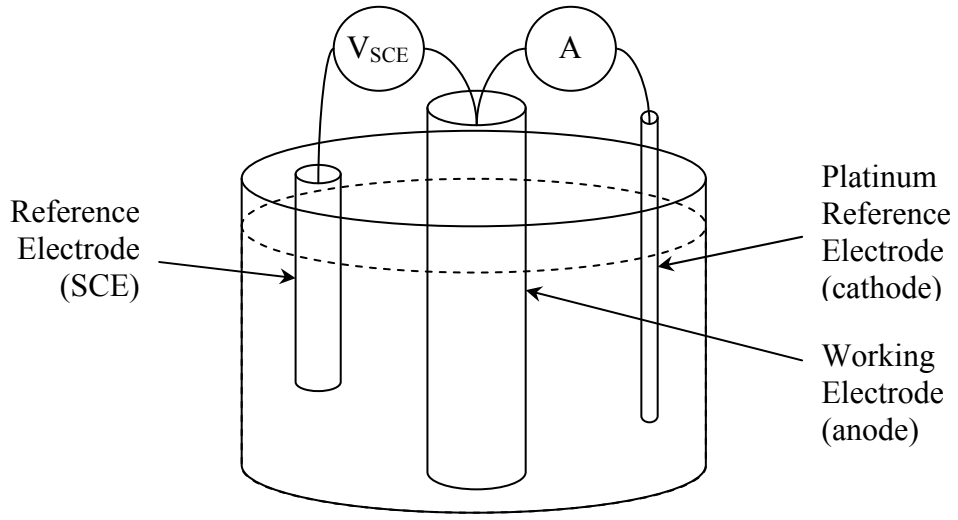

Figure 3-3: Simple System Setup

Table 3-2: Common Reference Electrode Potentials vs. SHE

Reference Electrode	Half-cell Reaction	Potential (V vs. SHE)
Copper-Copper Sulfate (CSE)	$CuSO_4 + 2e^- = Cu + SO_4^{2-}$	+0.318
Saturated Calomel (SCE)	$Hg_2Cl_2 + 2e^- = 2Hg + 2Cl^-$	+0.241
Standard Hydrogen (SHE)	$2H + 2e^- = H_2$	0.000

3.2.4 Mixed Potential Theory

The basis of the mixed potential theory is the Butler-Volmer equation. Because the relationship between potential and current is not linear in corroding systems there must be some relation between the two. They are actually exponentially related as shown in Equation 3-3. This is the Butler-Volmer equation.

$$i = i_0 \left(e^{2.3\frac{\eta}{\beta_a}} - e^{-2.3\frac{\eta}{\beta_c}} \right) \qquad \textit{Equation 3-3}$$

where

i = current density (I/A, I is the current and A is the exposed area to the electrolyte)

i_0 = exchange current density (represents the current flow per unit area between products and reactants when the reaction is at equilibrium)

η = overpotential ($\eta = E - E_0$, E is the applied potential and E_0 is the equilibrium potential)

β_a & β_c = Tafel constants

A plot of the applied potential, E vs. the log of the current density, log (i) is shown in Figure 3-4. From this plot it is possible to calculate the Tafel Constants. The Tafel Constants are simply the slope of each leg of the graph.

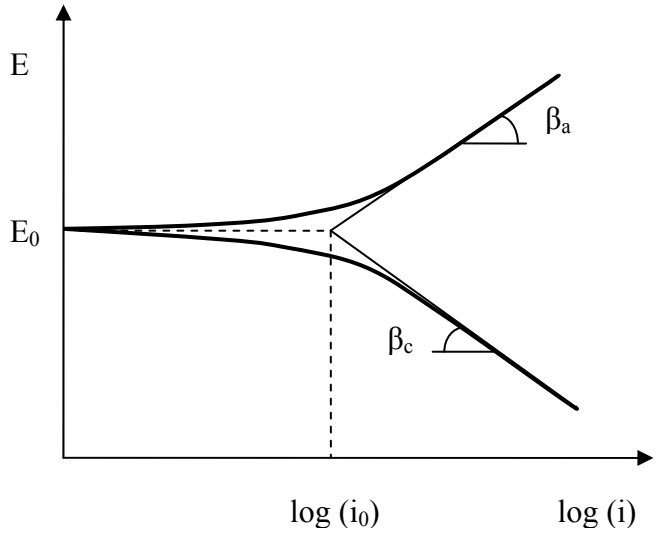

Figure 3-4: Semi-log plot of the Butler-Volmer Equation

The Butler-Volmer equation can be used to represent each half-cell reaction. When both reactions, anodic and cathodic are combined a mixed result is obtained where E_0 and i_0 become E_{corr} and i_{corr} respectively. This is known as the mixed potential theory. E_{corr} and i_{corr} represent the corrosion potential and the corrosion current density respectively for the entire cell. A plot showing the mixed potential theory can be seen in Figure 3-5. This plot illustrates the ideal mixed potential plot. In practice however this is never the case. There is an active, passive and transpassive range as shown in Figure 3-2. This affects the potentiodynamic curve and adjustments must be made to the value for i_{corr} and E_{corr}.

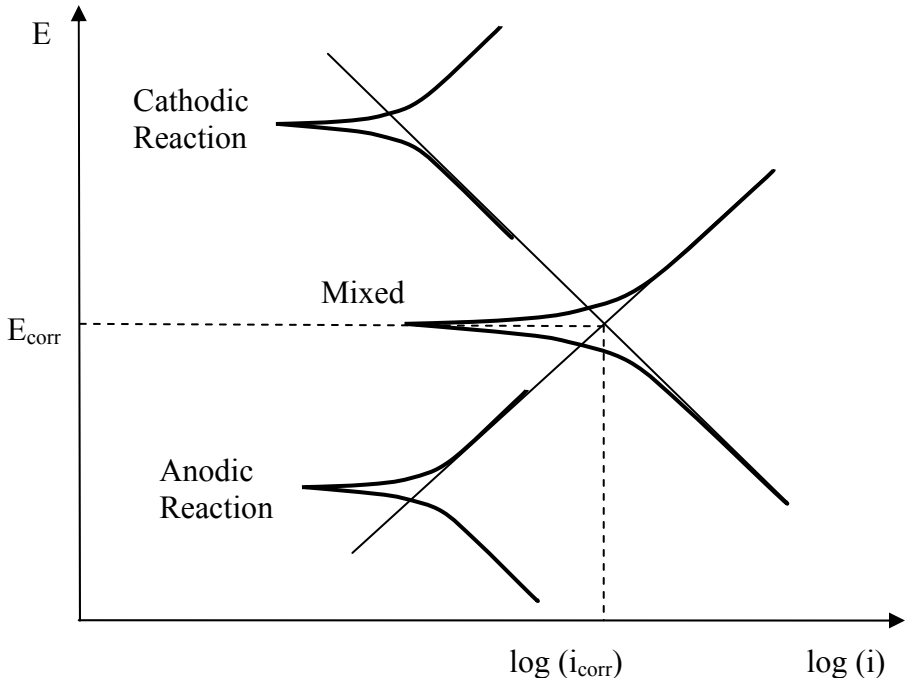

Figure 3-5: Mixed Potential Theory

3.3 CORROSION TESTING METHODS

Because of the electrochemical nature of corrosion, many electrochemical techniques are possible for the study of the different properties of metals and how they affect corrosion. The testing techniques explored in this thesis are DC or direct current techniques. These test methods are relatively simple to perform and to interpret. There are two types of DC techniques, controlled potential (potentiostatic) and controlled current (galvanostatic). This thesis will explore the controlled potential techniques. Controlled potential methods are much more common than controlled current methods. They involve applying a potential and measuring the current in the system. They are also most commonly used in laboratory and field applications. AC or alternating current methods are also used in corrosion testing. These methods are more involved and although they use the same variables as the DC techniques they must be analyzed in a frequency domain because of their time dependence.

In general the DC controlled potential methods discussed in this thesis require a potentiostat that polarizes the specimen. The potentiostat applies a potential to the system to force the potential away from the open circuit potential. This open circuit potential is the potential at which the system is in equilibrium and the anodic and cathodic reactions happen at equal rates. By forcing the potential to either the cathodic or anodic side, a net current flow is created to restore equilibrium. This current is measured and recorded. These two variables are used to develop a model of the specimen's corrosion behavior. The DC techniques explored in this thesis include Polarization Corrosion, Potentiostatic Corrosion, Potentiodynamic Corrosion and Linear Polarization Resistance (LPR) Corrosion.

3.3.1 Polarization Corrosion

As mentioned earlier it is possible to separate two half-cell reactions and measure the potential between them. This is the basis of the polarization corrosion method and is widely used in the field to monitor reinforced concrete structures. A common voltmeter can be used to take the readings. One lead from the voltmeter is attached to the corroding medium, the reinforcement. And the other is attached to a known half cell reaction, usually a SCE electrode. The measured potential difference can then be compared to a scale as shown in Table 3-3 to estimate if corrosion is occurring. Because it is two half-cell reactions and they must be in equilibrium before the potential reading is accurate, the leads must remain connected until the system becomes stable. This can take anywhere from a few minutes to several hours depending on the system.

Table 3-3: Probability of Corrosion Occurring (ASTM C876 1999)

E_{corr} (mV_{CSE}[1])	E_{corr} (mV_{SCE}[2])	Probability of Corrosion
More positive than -200	More positive than -123	Higher than 90% that no corrosion is occurring
Between -200 and -350	Between -123 and -273	Corrosion is uncertain
More negative than -350	More negative than -273	Higher than 90% that corrosion is occurring

[1] Potential is given in terms of the Copper-copper sulfate reference electrode
[2] Potential is given in terms of the Saturated Calomel reference electrode

3.3.2 Potentiostatic Corrosion

The potentiostatic corrosion method is one of the simpler tests to perform and is the basis of the DC corrosion tests. The one-step potentiostatic test only requires applying a single potential and measuring the current over a time period. This is the basis for the current accelerated corrosion tests (ACT). By increasing

the number of potential steps in a potentiostatic test it is possible to form a potentiodynamic curve. The current ACT tests require a specified applied potential be applied to the specimen. When the current value spikes then it means corrosion has started and the test is stopped. A typical plot of current vs. time for a potentiostatic corrosion test is shown in Figure 3-6.

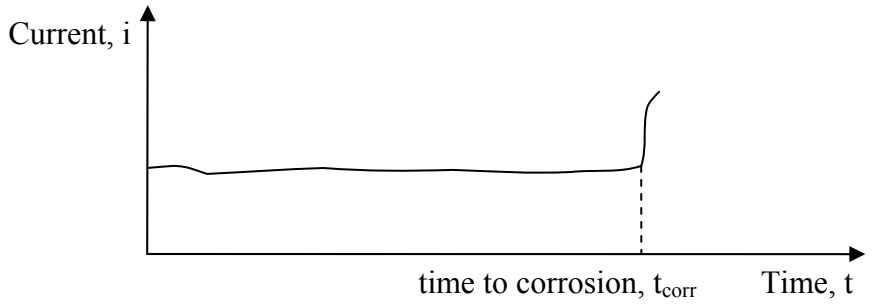

Figure 3-6: Typical plot from a potentiostatic accelerated corrosion test

3.3.3 Potentiodynamic Corrosion

The potentiodynamic corrosion test method requires the stepping of the potential applied to the specimen. The range of the potential steps depends on the specimen and also what part of the curve is needed. At each step the current value is recorded and a plot as shown in Figure 3-7 is made. The plot is usually semi-log because this gives the ability to obtain the Tafel constants easily. By using the potentiodynamic corrosion test method it is possible to get a complete description of what is happening. It is possible to get results in all ranges, the active, passive and transpassive. Because of this it is a highly popular laboratory test and in this case proved very important for this research.

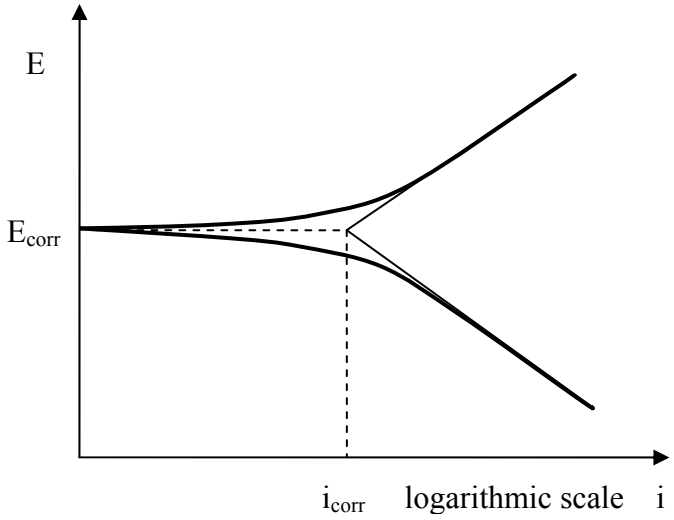

Figure 3-7: Idealized Potentiodynamic Polarization Plot

3.3.4 Linear Polarization Resistance (LPR) Corrosion

The linear polarization resistance corrosion tests use the same principle as the potentiodynamic tests. However there is less of a potential range scanned, usually ±20 mV. Not only does this allow for quicker testing it also allows the specimen to be tested without exposing it to the entire range of potentials. By not exposing it to the range the specimen is not damaged and can be tested again. This method is now commonly used in the field.

The polarization resistance is defined as the slope of the curve at the origin, independent of the degree of linearity. $R_p = \Delta E/\Delta i$ as shown in Figure 3-8. It has been established that the polarization resistance, R_p is inversely proportional to the corrosion rate. This corrosion rate depends on i_{corr} and Equation 3-4 has been established to relate the two. As seen in the equation R_p is also related to the Tafel constants β_a and β_c. These constants usually range from 112 to 224 mV for concrete structures but because there is different materials being tested the Tafel constants had to be calculated from the potentiodynamic plots.

$$R_p = \frac{\beta_a \beta_c}{2.3 i_{corr}(\beta_a + \beta_c)}$$ ***Equation 3-4***

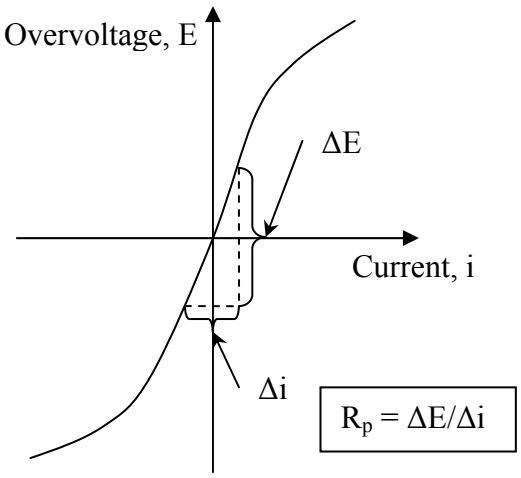

Figure 3-8: Typical Plot of LPR Test

3.4 POSSIBLE ERRORS IN CORROSION TESTING

As with all electrochemical testing there can be some error involved. In previous research done by Hamilton[12], Koester[16], Schokker[23] and Pacheco[18] it was noticed that ohmic electrolyte resistance was a factor in the accelerated testing of grout. In any electrical circuit the various pieces comprising the circuit all have an internal resistance. The same is true for an electrochemical circuit. The resistance of the wiring and the metal specimens is negligible in comparison to the other aspects of the testing. The electrolyte (salt water in this case) and the grout that encases the strand are not as conductive as the rest of the system. The electrolyte remains the same for all experiments so that it does not affect the result. In previous testing it was noticed that different grouts provided different resistances[12, 16, 23 & 18]. It was important to correct for this so that the comparisons would not be flawed. In this research the grout used was the same for the

comparison tests. Also although the strands have different diameters this was taken into account when designing the specimens. The cover on each strand type was kept the same so that the ohmic resistance would be the same for all strand types and would not have to be considered in the results.

3.5 ACCELERATED CORROSION TESTING

The currently accepted accelerated corrosion testing method was developed by Thompson, Lankard and Sprinkel[26] and was perfected by Hamilton[12], Koester[16], Schokker[23] and Pacheco[18]. It is used to compare grouts for use in post-tensioning systems. As mentioned earlier it uses the potentiostatic corrosion technique. Using a potentiostat, a steady potential of +200 mV_{SCE} is applied to the specimen. The current in the system is monitored. When the current has spiked corrosion has initiated. This time is defined as the time to corrosion time. For a grout to be used in the field the time to corrosion time must be greater than 1000 hours or 42 days as recommended by PTI 2003.

This technique is very time consuming. From the research done by Schokker and Pacheco it has been shown that by using the Linear Polarization Resistance (LPR) technique it is possible to get a comparison between the grouts[18, 19]. It has been found that the polarization resistance and the corrosion rate are proportional to the time to corrosion. The linear polarization resistance technique also takes considerably less time to complete and uses the same equipment. Currently there is a proposal being balloted in PTI made by Schokker to make this polarization resistance technique a recognized accelerated corrosion testing technique[24].

CHAPTER 4
Accelerated Corrosion Testing

4.1 INTRODUCTION

From the previous project it was noticed that there was a need for early testing of the new post-tensioning systems[22]. Because substantial research has already been done in the grouting area it became apparent that the next step would be to test the strands[12, 16, 18 & 23]. It was important that the strands be tested in the same form as they are in the field. That is they should be encased in grout and exposed to a salt water solution. The accelerated corrosion testing methods mentioned in the previous chapter worked well for estimating the time to corrosion for different grout types. So the techniques were applied to compare the different strand types. The goal was not to get exact times to corrosion but to compare the different strand types side by side and rate them.

This chapter will also outline the development and manufacturing of the specimens used for testing as well as the test setup and procedures used. It should be noted that the specimen design and testing were very similar to that used by Schokker[23] and Pacheco[18].

4.2 POTENTIOSTATIC ACCELERATED CORROSION TESTING

The standard method for testing grout was mentioned in the previous chapter. It basically involves applying a fixed potential of +200 mV_{SCE} to the specimen immersed in a salt solution and waiting for the observed current in the circuit to spike[19]. The current spike means that corrosion has initiated and the time till this happens is considered the time to corrosion. The grouts are then rated according to their time to corrosion. A typical current vs. time plot for an

accelerated corrosion test is shown in Figure 4-1. These tests are very time consuming and can take many weeks before results are known.

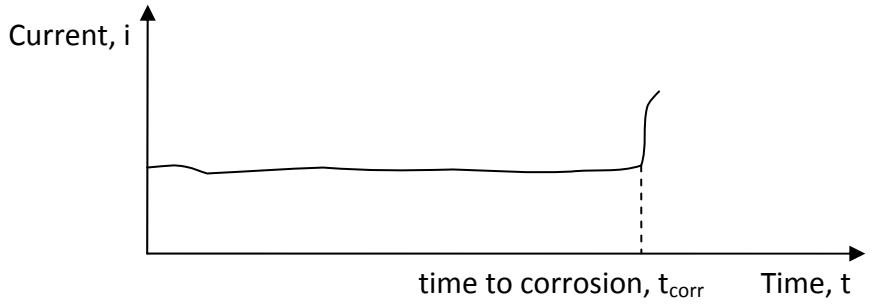

Figure 4-1: Typical plot from a potentiostatic accelerated corrosion test

The +200 mV_{SCE} was specified by Schokker[23], down from the initial +600 mV_{SCE} specified by Hamilton[12]. This value was chosen because it falls in the passive range of steel encased in grout and this is the common range that the prestressing strand is within in service. Also it was initially thought that the grout needed to be pre-cracked[12]. Pre-cracking gave the salt solution a quick path to the strand. This idea was dismissed because the pre-cracking just increased the variability of the test results. So the standard accepted accelerated corrosion tests done today require that the specimens be crack and defect free, and the tests must be run at +200 mV_{SCE} until corrosion has initiated.

Initially it was thought that this test would be suitable for testing the different strand types. An attempt was made to adapt this potentiostatic accelerated corrosion test to the strand tests. However in order for the test to be successful the specimens would have to be run at the same overvoltage, that is, the potential picked for each strand type would have to be the same. Another thought to make the tests successful was to pick a different overvoltage for each strand type that fell within the passive range for that particular strand. However it

would have been very difficult to justify the overvoltage chosen and the results would be very skewed depending on the overvoltage chosen. In the previous chapter the potentiodynamic testing was mentioned and one of its attributes is the ability to show the corrosive behavior of the material over its entire range. It was therefore decided that three potentiodynamic tests for each strand type be run to establish the corrosive behaviors.

What was observed was a high variability in the potentiodynamic plots. A potentiodynamic plot showing one test from each strand type is shown in Figure 4-2 for reference. From this initial test it was established that the potentiostatic test would not be a feasible option and would not give accurate results. The main reason was that there was no single potential that fell within each strands passive range. Also there would be no justification for picking a different potential for each strand type because the results would be highly dependent on the potentials chosen.

The potentiostatic corrosion tests were thereby discarded as an equitable form of comparing the different strand types.

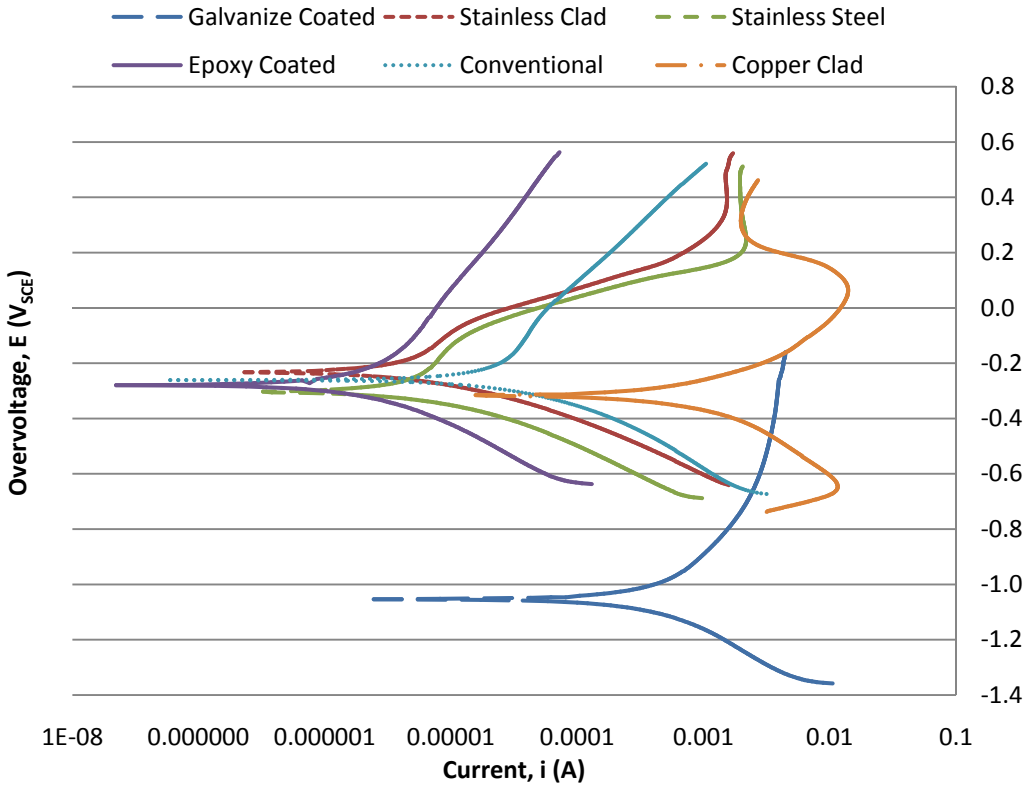

Figure 4-2: Potentiodynamic plots for all strand types

4.3 LINEAR POLARIZATION RESISTANCE CORROSION TESTING

Currently Schokker has a ballot proposal with the PTI (Post-Tensioning Institute) for a change to the accepted accelerated corrosion testing method[24]. If passed, it will allow the accelerated corrosion tests to be done using the linear polarization resistance technique. This technique will greatly reduce the time required for testing grouts. The technique is outlined in the previous chapter. A correlation between the polarization resistance, R_p for the specimens measured using the linear polarization resistance test and the time to corrosion was found (see Pacheco 2003). It is a linear relation where $t_{corr} = 1.25\ R_p$, where t_{corr} is in

hours and R_p is in $k\Omega cm^2$. Also noted is that this method works well for grouts with low to average corrosion protection[18].

The goal of the rest of this research is to adapt this testing technique to compare the times to corrosion for the different strand types.

4.4 TESTING PLAN

Six different strand types were tested. For each strand type, 10 potentiodynamic and 10 linear polarization resistance tests were performed. The different metal types had varying properties so it was decided that 10 tests would be enough to control the variability of electrochemical tests and to get accurate results. The same specimens were used for both the linear polarization tests and the potentiodynamic tests. This was possible because the potential range that the specimens were exposed to during the linear polarization tests is very small, ±20 mV. This range does not polarize and damage the specimens, so it was possible to use the same specimens to conduct the potentiodynamic tests once the linear polarization tests had been completed. A list of the strands tested including their diameters and the test identifiers are listed in Table 4-1. Note that only one conventional strand type was used as opposed to the 2 used for tension testing. Since most standard conventional strands have similar chemical properties it was decided that only one was needed for comparison. The 0.6 in. strand was chosen because it was a much newer strand and did not have visible signs of corrosion on its surface due to exposure to the atmosphere.

Table 4-1: Testing Plan

Type	*Nominal Dia. (in)*	*Area (in^2)*	*Potentiodynamic Test Identifier*	*LPR Test Identifier*
Epoxy Coated	0.5	0.153	PD-(1-10)*-EC	LPR-(1-10)*-EC
Conventional	0.6	0.220	PD-(1-10)*-CN	LPR-(1-10)*-CN
Hot Dip Galvanized	0.5	0.152	PD-(1-10)*-GC	LPR-(1-10)*-GC
Stainless Clad	0.6	0.217	PD-(1-10)*-SC	LPR-(1-10)*-SC
Stainless Steel	0.6	0.221	PD-(1-10)*-SS	LPR-(1-10)*-SS
Copper Clad	0.5	0.144	PD-(1-10)*-CC	LPR-(1-10)*-CC

* (1-10) being the test number

4.5 SPECIMEN DESIGN

The design of the specimens is very similar to that done by Pacheco[18]. However to accommodate the different strand sizes there needed to be some modifications to the specimens used in the standard accelerated corrosion tests. The specimens were designed to expose a fixed area of grout to the electrolyte, salt solution. Clear tubing was used so that the inside was visible while casting which helped to avoid defects in the area that would be exposed. Defects may greatly affect results in the potentiostatic tests because the tests are based on how long it takes for the electrolyte to make it through the grout cover to the strand surface. The linear polarization resistance and the potentiodynamic are not as affected by defects and small defects can be tolerated. The two specimens are shown in Figure 4-3.

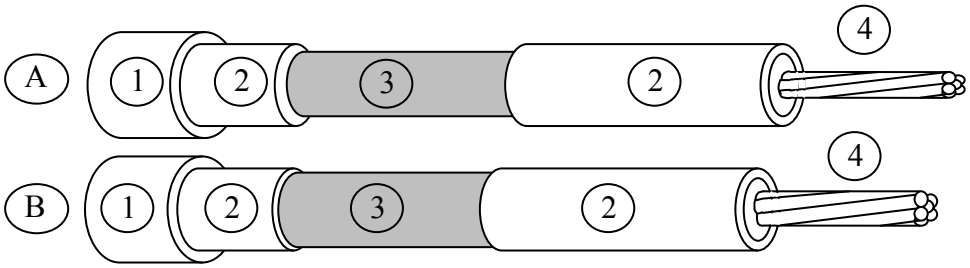

A: specimen for 0.5 in strands
1. 25.4 mm (1 in) PVC end cap
2. Clear PVC tubing: 50.8 mm (2 in) in end cap & 101.6 mm (4 in)
3. Exposed Grout: 25.4 mm (1 in) dia., length 90 mm (3.5 in)
4. 12.7 mm (0.5 in) prestressing strand: length 305 mm (12 in)

B: specimen for 0.6 in strands
1. 25.4 mm (1 in) PVC end cap
2. Clear PVC tubing: 50.8 mm (2 in) in end cap & 101.6 mm (4 in)
3. Exposed Grout: 28 mm (1.1 in) dia., length 81.3 mm (3.2 in)
4. 15.2 mm (0.6 in) prestressing strand: length 305 mm (12 in)

Figure 4-3: Specimen Design

The strands that were provided had a natural curvature from being rolled up. It was possible to get them basically straight by bending them without heat using an aluminum pipe and a table vise. However after straightening the strands were not perfectly straight. So to be sure that the strands would be centered where it was most important, that is, the exposed area, the spacers were moved. The spacers that were used to keep the strand centered were moved to 0.5 in. from the edges of the exposed section. These spacers were made using 1/16 in. acrylic rods. The 1 in. PVC tubing was drilled and the rods were inserted to make a grid pattern. Where the rods protruded from the PVC tubing a quick dry epoxy was used to seal this location. By sealing it with epoxy the electrolyte was not able to flow along the acrylic/grout joint to the strands. A diagram of the acrylic rod spacer is shown in Figure 4-4.

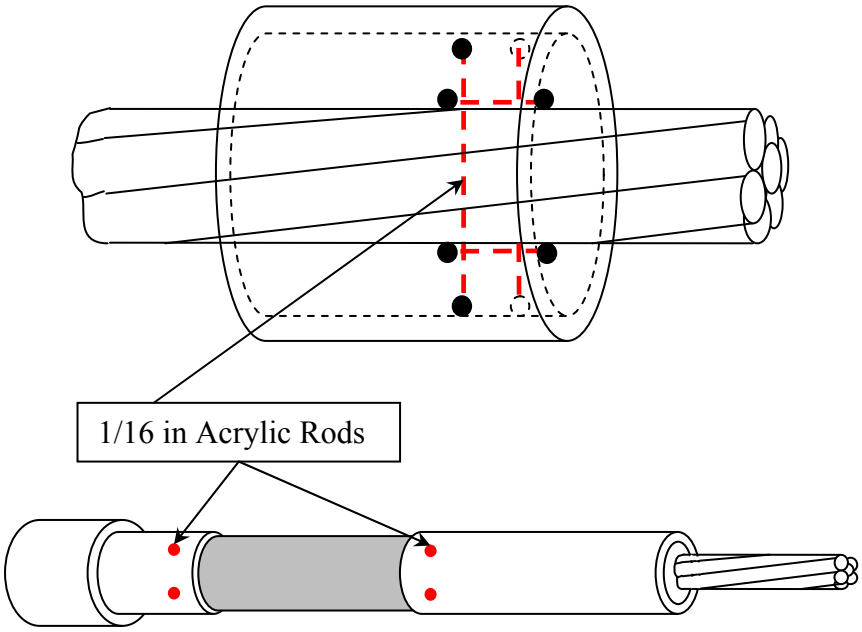

Figure 4-4: Diagram of acrylic rod spacer design showing position on specimen

For the 0.6 in. strands it was important that they maintain the same cover so that the tests would be comparable and ohmic electrolyte resistance would not be a factor. Because the PVC tubing manufacturers do not manufacture PVC to custom internal diameters the same PVC tubing had to be adjusted. The 0.6 in. strand specimens needed to have an internal diameter that was 0.1 in. larger than the 0.5 in. strand specimens. This was achieved by machining the inside of the tubing using a lathe. For continuity, and to be sure that no cracking formed at the point where the exposed surface started, the PVC directly adjacent to the exposed area was also machined to the same diameter.

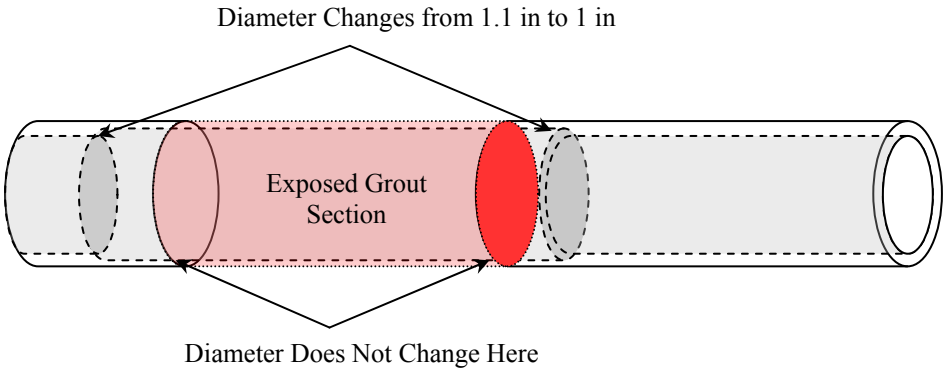

Figure 4-5: Diagram showing how the tubing for the 0.6 in strand specimens was machined

4.6 SPECIMEN MANUFACTURE

The PVC casing and the strand pieces had to be prepared first. Once everything was assembled and water tested the specimens were cast. The steps are outlined in the following sections.

4.6.1 PVC Casing Preparation

The clear PVC pipe was delivered in 5 ft. lengths. They were cut in half using a table saw to be more manageable. In order for the faces of the pieces to be very smooth and fit together well all of the PVC pieces were cut using a lathe as shown in Figure 4-6. The same lathe was used to machine the inside of the 0.6 in. strand PVC casings to the larger diameter. When the inside of the PVC casings was machined, the PVC did not remain clear but became slightly more opaque. However it was still possible to see the grout when it was cast. After all the pieces had been cut the next step was to groove the part that would be removed to expose the grout. By cutting a groove in the PVC in this area it was possible to remove the PVC casing quickly and easily when it was time to test. No grinders or lathes were needed in the removal of the PVC section. A Lagun Republic milling

machine was used to cut the groove in the PVC (see Figure 4-7). By using a milling machine the groove was able to be cut as deep as possible for easier removal after casting. Figure 4-8 shows the inside and outside of the machined part. Notice the groove that has already been cut.

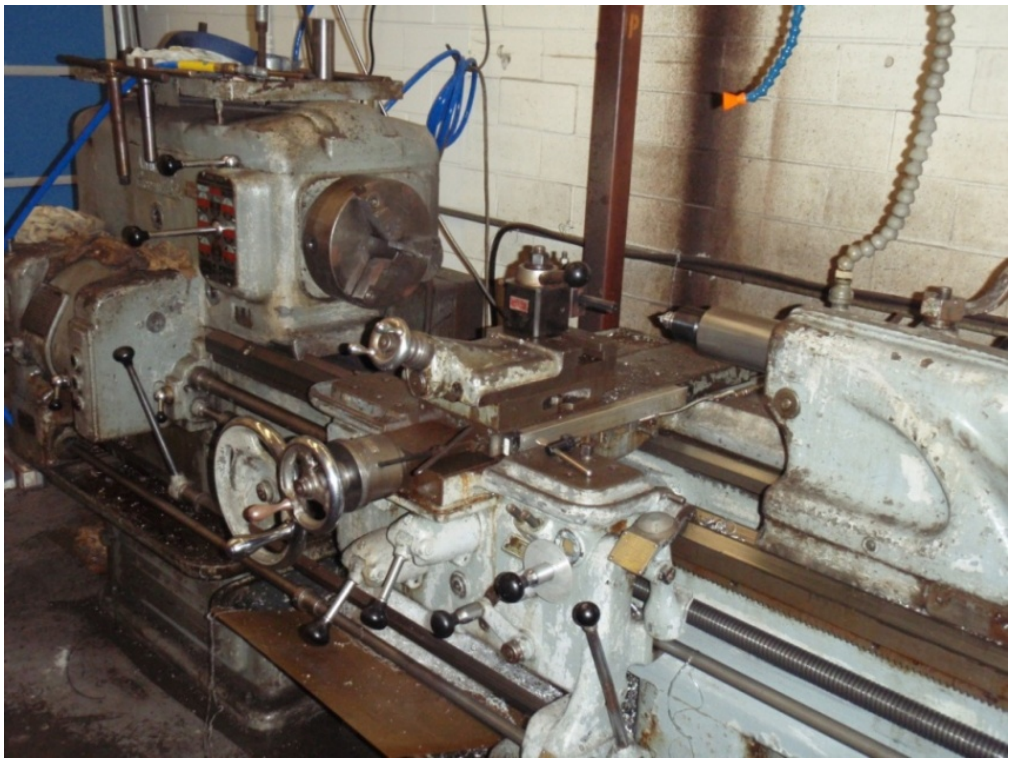

Figure 4-6: Lathe used in preparing PVC casings

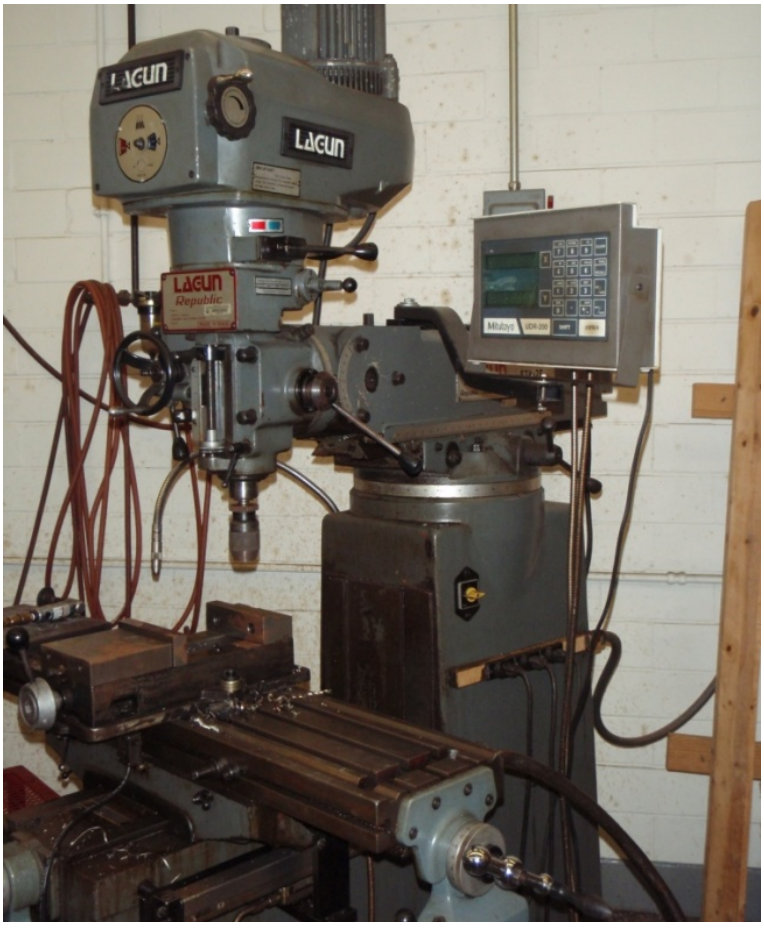

Figure 4-7: Lagun Republic milling machine

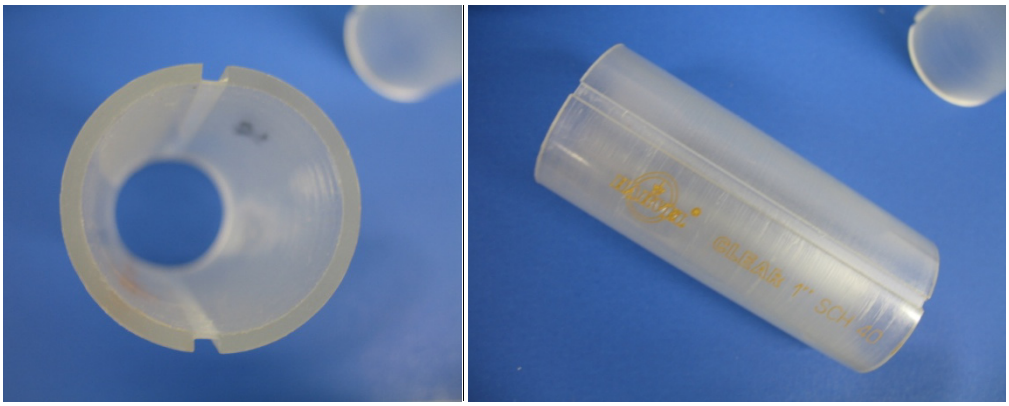

Figure 4-8: Inside and outside out machined part

The next step was to drill the holes in the two other PVC parts. These holes would be used to put the acrylic rods that were necessary to center the strands. This was followed by the application of a fast drying epoxy to seal the holes and to hold the acrylic rods in place. Figure 4-9 shows a top view of the grid created with the acrylic rods and the epoxy used to seal the holes. Notice in Figure 4-9 that you can see the step from a 1.1 in. diameter to a 1.0 in. diameter as mentioned earlier. This picture was taken of one of the 0.6 in. strand specimen parts.

Figure 4-9: Specimen part showing acrylic rods and epoxy

4.6.2 Strand Preparation

The strands were cut using an abrasive cut-off saw as seen in Figure 4-10. Also shown in Figure 4-10 is the bench grinder that was used to bevel the ends of the strand so that they fit easily into the acrylic rod spacers. This saw cuts the strands extremely fast and although the strand becomes heated at the point where it is cut the heat dissipates rapidly. Also the testing or exposed area did not become hot while the strand was cut. This was important because heat may change the properties of the strand. Some of the strand types had natural curvatures that would have made it impossible to cast them in the specimens. To fix this they were straightened using an aluminum pipe and a table vise. No heat was used to straighten them.

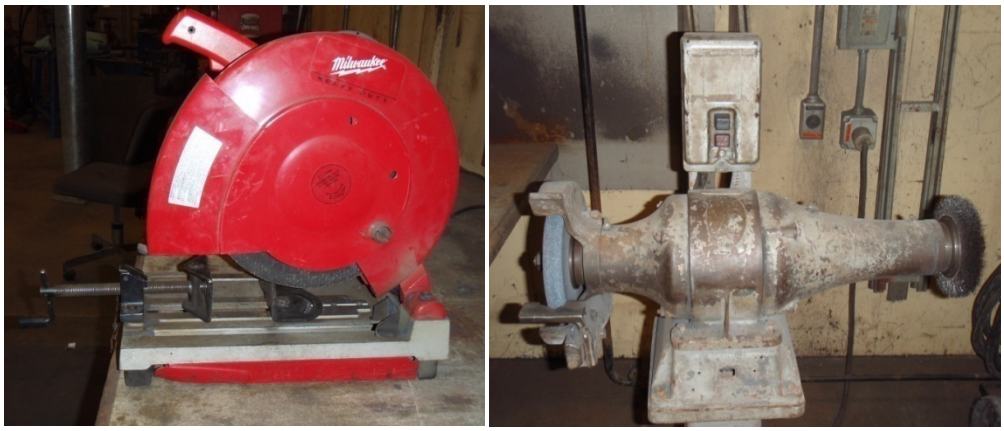

Figure 4-10: Abrasive cut-off saw and bench grinder

One of the strand types had to be prepared a little differently. The flow filled epoxy coated strand is completely coated and if the coating is not damaged there will be no chance for corrosion. Therefore the surface had to be intentionally damaged for the strand to be tested. This was done by placing the strand in the tension testing machine and using the end chucks. The teeth in the chucks

embedded themselves in the epoxy and exposed the steel below. This was considered to be an accurate way of representing the damaged epoxy because this would happen at the ends of the strand in the field when the strand is stressed. An example of the damaged epoxy is shown in Figure 4-11 and the chuck used to cause the damage is shown in Figure 4-12.

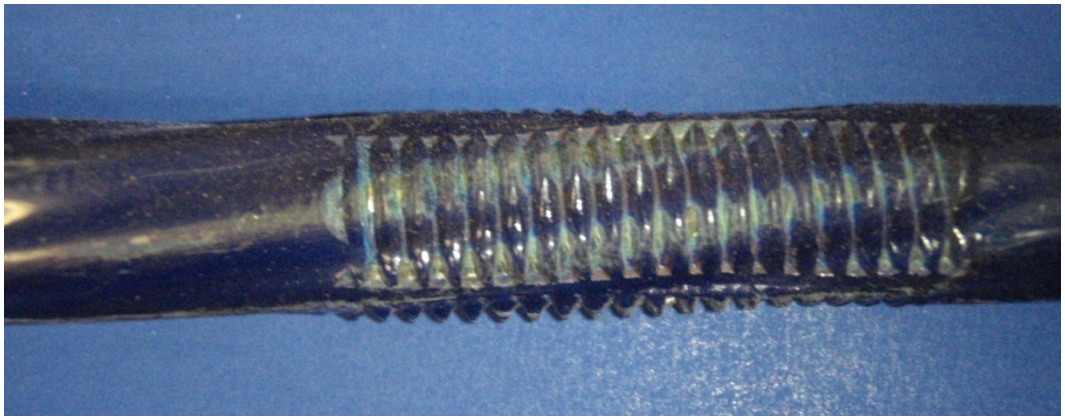

Figure 4-11: Flow filled epoxy coated strand showing damage done by chuck

Figure 4-12: Chucks used to damage epoxy coating

Finally the ends of the strand that would be sticking out of the specimens were taped with duct tape. This prevented the ends from being exposed to

moisture in the moist room while curing. If the strands were exposed to the moisture, corrosion on the ends would have been a problem.

4.6.3 Parts Assembly

The PVC end caps were first stuck to the smaller pieces of PVC tubing using regular PVC cement. All of the PVC parts were then glued together using an adhesive silicone. This would allow for easy removal of the PVC casing in the area to be tested. Because the PVC parts were cut using the lathe all the parts fit together perfectly and there was very little silicone needed to make the connections. This also allowed the silicone to dry and be sturdy without using tape to hold the parts together. Figure 4-14 shows the silicone used and also an assembled PVC casing.

Figure 4-13: Adhesive silicone and assembled PVC casing

Before the PVC casings could go into the last casting stage they had to be tested. Each casing was water tested to be sure that the grout would not leak out during casting or curing.

4.6.4 Casting

The specimens were cast over a period of a week and a half. A total of 10 specimens were cast per day. All 10 specimens cast each day contained the same strand type. The SikaGrout 300 PT was used. This grout was chosen because it is a premixed, non-bleed, high flow grout. The water to cementious materials ratio was taken as 0.3. This produced a grout that flowed easily and was also not very watery. The grout was mixed in a 5 gallon bucket with a high shear blade attached to a variable speed mixer for the required amount of time. It was poured into each specimen and the specimens were agitated to minimize air bubbles. Figure 4-15 shows the apparatus used for casting.

Figure 4-14: Apparatus used for casting

4.6.5 Curing

After casting the specimens were placed in containers to hold them upright. Each container held 5 specimens and was labeled with the strand type, date of casting and date of testing. The containers were then placed in a moist

room to cure for 28 days. By curing for 28 days it reduced possibility for variability of results.

4.7 TESTING EQUIPMENT SETUP / TEST PROCEDURE

4.7.1 Testing Equipment Setup

The testing done at The Pennsylvania State University by Schokker and Pacheco[18] was done using equipment supplied by Gamry Instruments. The equipment was highly recommended for its simplicity and software. So for the testing done on this project the same type of equipment was used. The test setup used was the same as that used for performing a standard accelerated corrosion test. The setup used for the testing done at The University of Texas at Austin is outlined below.

It consists of a potentiostat connected to a computer and a standard corrosion cell. In this case the potentiostat was built into the computer. The potentiostat was supplied by Gamry Instruments and was installed in a HP Compaq computer. The Series G 750™ Potentiostat/Galvanostat/ZRA was installed and setup by Gamry Instruments. Also supplied by Gamry was an Electrochemical Multiplexer that is used to perform multiple tests at a time. A picture of the computer and the multiplexer is shown in Figure 4-16.

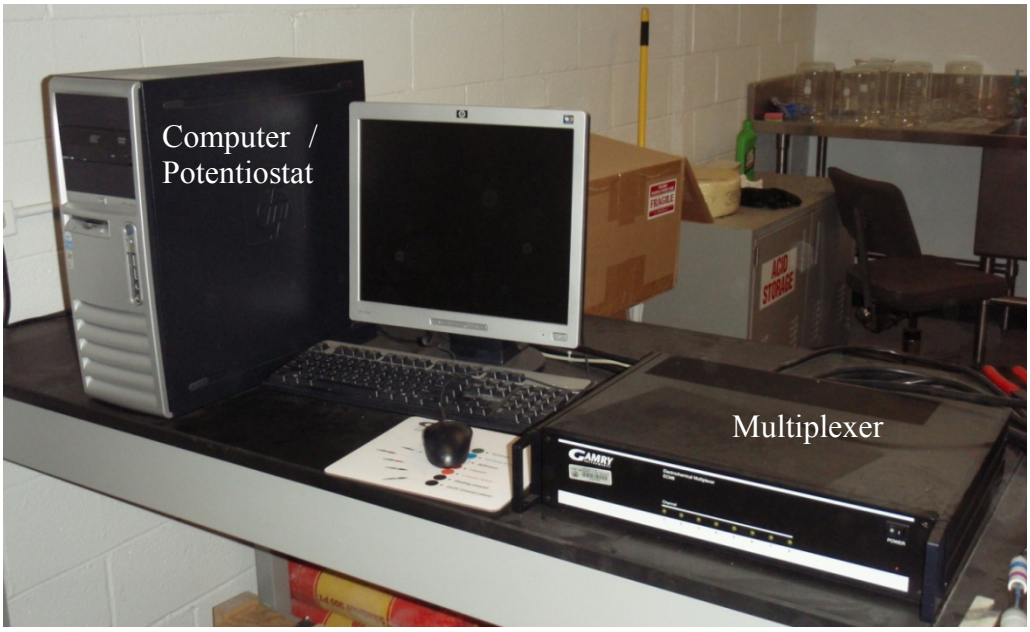

Figure 4-15: Computer, potentiostat and multiplexer

The potentiostat is connected to a standard corrosion cell used for corrosion testing. The corrosion cell is shown in Figure 4-17. The cell is made up of 3 different electrodes immersed in an electrolyte, all contained in a beaker. The beaker is also covered to prevent outside elements from falling into the beaker and to support the reference and counter electrodes. There is a working electrode (strand specimen), a counter electrode (platinum coated wire) and a reference electrode (SCE). The electrolyte is a 5% NaCl solution.

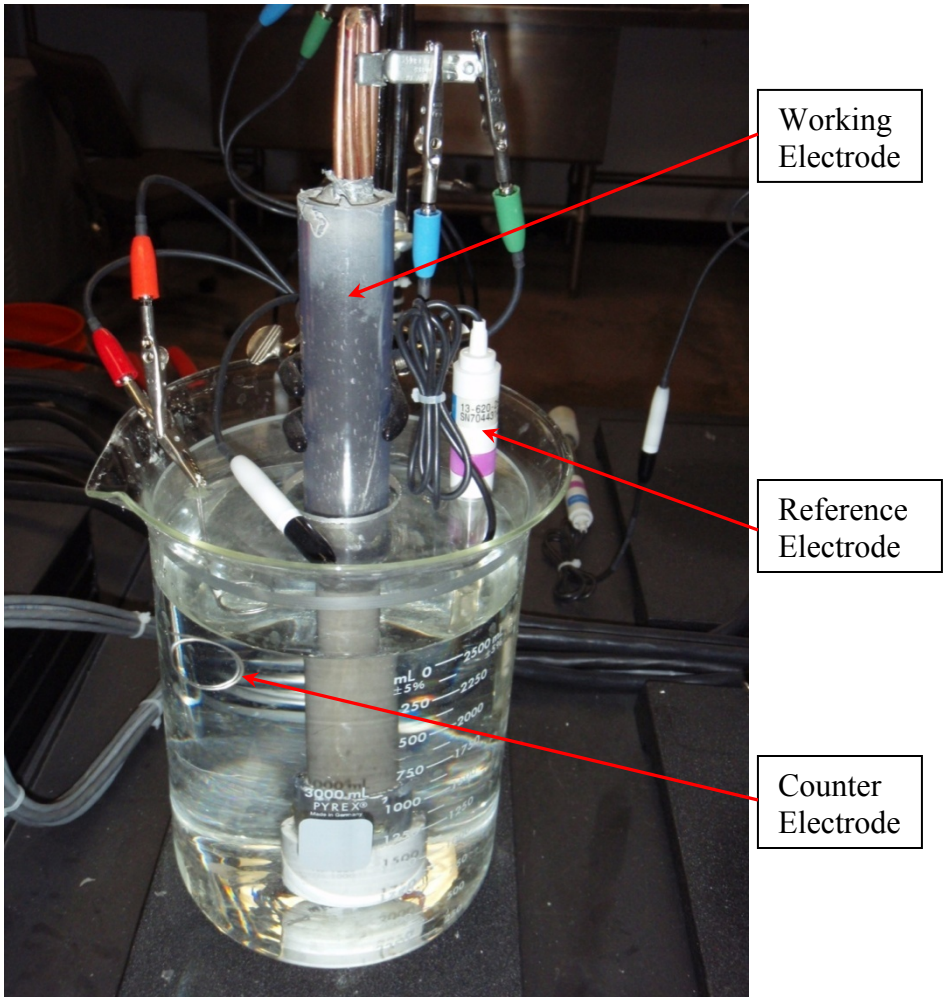

Figure 4-16: Corrosion cell

The working electrode is the specimen being tested. In this case it is the prestressing strand encased in grout. The counter electrode was supplied by Anomet Products & Supercon Inc. It was a 0.05 in. diameter platinum clad wire. As shown in Figure 4-18 the platinum coated wire was bent so that none of the cut ends of the wire would be exposed to the electrolyte. This was done because the ends, when cut do not have platinum coating the internal wire. Therefore the internal wire would be exposed to the electrolyte and would corrode because it is

not as noble as platinum. The counter electrode was then fixed to the cover for the beaker using a quick dry epoxy. This helped protect the ends even more from getting exposed to the electrolyte.

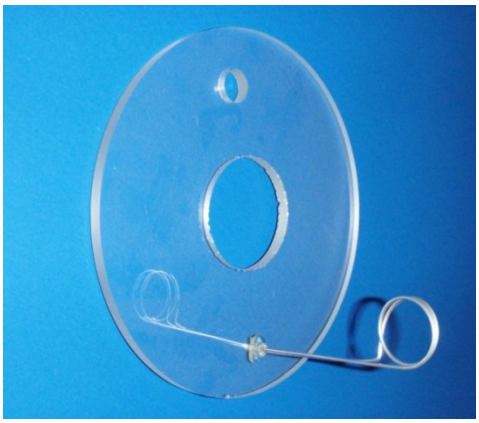

Figure 4-17: Cell cover with counter electrode attached

The reference electrode was manufactured by Fisher Scientific and was a saturated calomel electrode (SCE). It was a plastic, gel filled electrode which does not need maintenance. The electrode is shown in Figure 4-19.

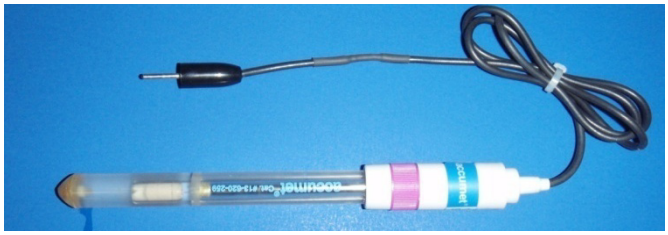

Figure 4-18: Saturated calomel reference electrode

4.7.2 Test Procedure

As stated earlier the linear polarization resistance tests were done before the potentiodynamic tests. Table 4-2 outlines the variables used in each of these tests.

Table 4-2: Testing variables

	Linear Polarization Resistance	*Potentiodynamic*
Initial E (mV) vs. E_{oc}	-20	-500
Final E (mV) vs. E_{oc}	20	500
Scan Rate (mV/s)	0.5	0.5
Sample Period (s)	0.2	5

Once all the specimens had cured for 28 days in the moist room they were removed for testing. The PVC casing was removed from the exposed area. Figure 4-20 shows the specimen before and after the casing was removed.

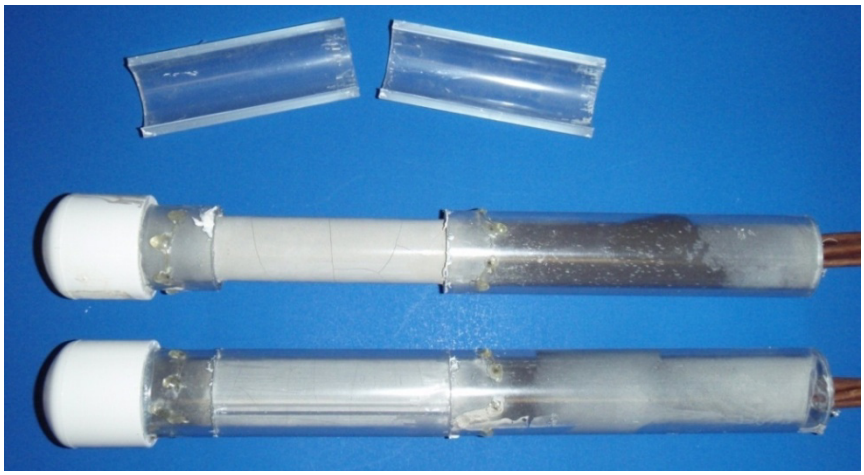

Figure 4-19: Specimen before and after casing was removed

The specimen was then immediately placed in the cell and connected to the potentiostat. The cell contained the electrolyte which was made up of distilled water mixed with salt (NaCl) 5% by weight. Shown earlier in Figure 4-17 is the specimen immersed in the cell and connected to the potentiostat for testing. Each test period, that being the LPR test and the potentiodynamic test lasted for approximately 1 hour.

CHAPTER 5
Results and Analyses of Corrosion Tests

5.1 OVERVIEW

Two different electrochemical test methods were used to establish the corrosive properties of the strand specimens. Linear polarization resistance tests were run first. The results from these tests were used to compare the times to corrosion of the different strand specimens. The reasoning behind the use of this particular test was outlined in the previous chapter. A potentiodynamic test was then run on each specimen after the linear polarization resistance test had been completed. It was established that the linear polarization resistance tests were to be used as the main tool for comparison of the strand specimens. Therefore the potentiodynamic tests were only performed to illustrate how the different strand types have different active and passive ranges. They also showed how variable these ranges could be even from one specimen to the next of the same strand type. This helped to support the reasoning behind the abandonment of the potentiostatic accelerated corrosion test as an appropriate test for this study.

The results of the two testing procedures are shown in the following sections. The plots of all ten potentiodynamic tests are shown for each strand type on a single figure. This is important to show the extent of the variability of the test results. It also allows for the pinpointing of outlying results. The linear polarization resistance test results are also shown in the same manner. Most important are the slopes of the linear polarization resistance test plots at the point where the current density is equal to zero. This slope is the polarization resistance, R_p used to compare the times to corrosion of the strand specimens. By putting all ten linear polarization resistance test results on one plot it is easy to compare the

slopes of the plots of the different tests. Once again outlying results can be identified and ignored. The results of the linear polarization resistance tests are also shown in a table for easy comparison. An analysis region of 5 mV above and below E_{corr} was used to determine the value of the polarization resistance, R_p. This analysis region corresponds to the range about the corrosion potential, E_{corr} which was considered approximately linear for the calculation of R_p. The E_{corr} values that are listed in the results were obtained from the polarization resistance tests and in some cases do not match the potentiodynamic test results. However because the polarization resistance tests were performed first the E_{corr} values from these tests were used.

In these electrochemical tests it is difficult to establish a set value for the actual area that is involved in the test circuit. When the specimen is initially immersed into the electrolyte, only the grout in the exposed area has direct contact with the electrolyte. It is not trivial to think that as time passes in the test that the electrolyte can in fact travel between the grout surface and the PVC. This makes it very difficult to determine how much of the working electrode is in fact exposed to the electrolyte. However this is a comparative study and all the areas remain the same. Also it was assumed that since all the tests took the same amount of time that the electrolyte would have traveled the same amount in each test. Therefore for ease of calculation only the exposed area was used in calculation of the current density. The same area was used for the calculations in the linear polarization resistance tests and the potentiodynamic tests.

5.2 CONVENTIONAL

The conventional strand specimens were tested to establish a base to compare the other strand types. In an ideal setting the grout encasing the conventional strand keeps the strand protected. It helps the surface to form a

passive film and the surface becomes more stable. This was explained in Chapter 3. It was thus expected that there would not be much variability between the results for the ten conventional strand tests.

5.2.1 Potentiodynamic Tests

The plots for all ten potentiodynamic tests that were performed on the conventional strand specimens are shown on a single graph in Figure 5-1. There was very little variability in the potentiodynamic plots. The E_{corr} values varied from -558 mV_{SCE} to -648 mV_{SCE}. From the potentiodynamic plot it can be noticed that the assumption that the conventional strands are in a passive state while encased in grout is in fact true. The strand actually remains in a passive state throughout quite a large range of potentials.

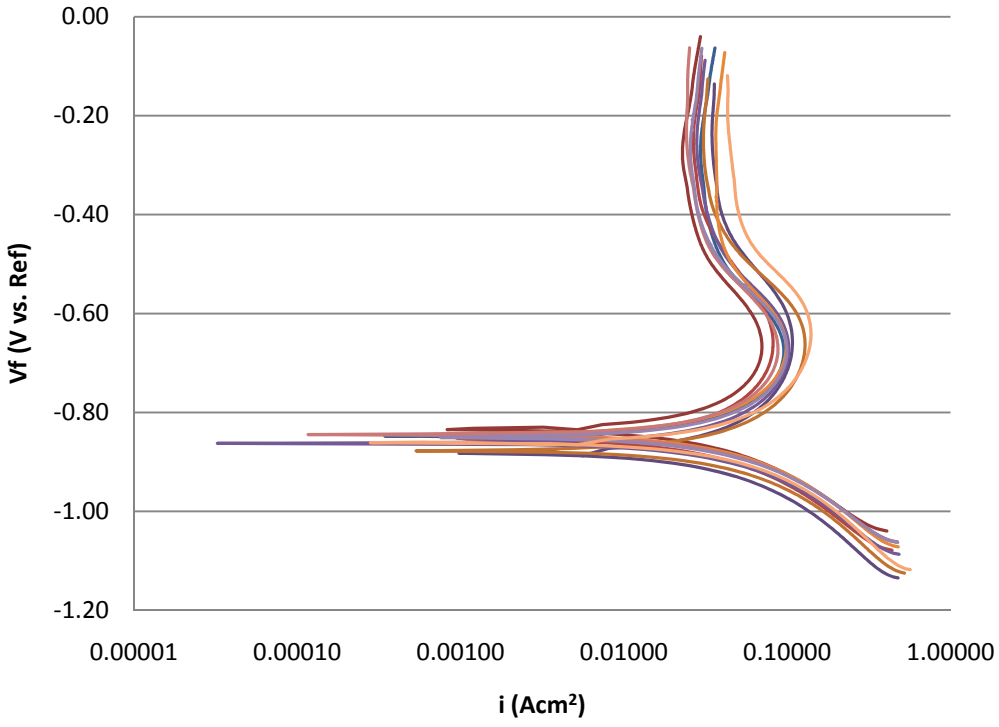

Figure 5-1: Potentiodynamic plot of conventional strand tests

5.2.2 Linear Polarization Resistance Tests

The results of the linear polarization resistance tests performed on the conventional strand specimens are shown on a single plot in Figure 5-2. Although the results look scattered they do not actually have much variability. It just seems that way because of the expanded scale of the y-axis.

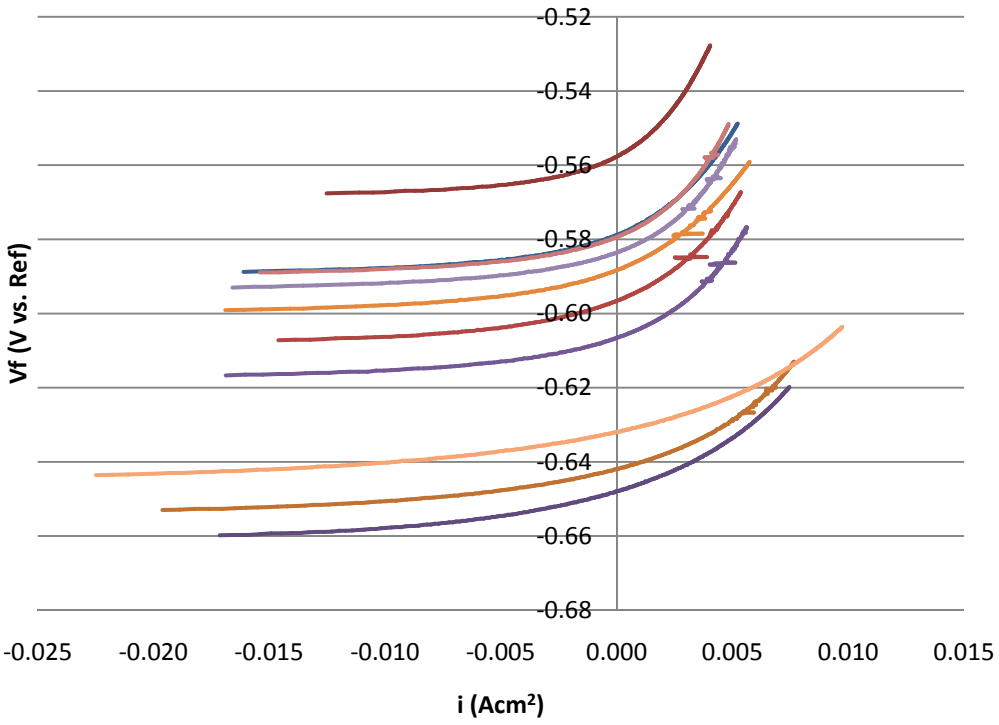

Figure 5-2: Linear polarization resistance plot of conventional strand tests

The low variability is also reflected in the values of the polarization resistance. There are no dramatically outlying values therefore an average of all the tests will best represent the actual polarization resistance. The average

polarization resistance, $R_{p\ AVG}$ = 10.82 kΩcm^2 and the average corrosion potential, $E_{corr\ AVG}$ = -601 mV_{SCE}. Table 5-1 lists the values for both the polarization resistance and the corrosion potential for all ten tests performed.

Table 5-1: Linear polarization resistance results for conventional strand tests

	Test 1	*Test 2*	*Test 3*	*Test 4*	*Test 5*	*Test 6*	*Test 7*	*Test 8*	*Test 9*	*Test 10*
Polarization Resistance, R_p (kΩcm^2)	11.83	15.46	9.371	7.967	11.99	10.56	11.79	11.80	10.74	6.723
Corrosion Potential, E_{corr} (mV vs. ref)	-579	-558	-648	-642	-597	-607	-588	-579	-584	-632

5.3 COPPER CLAD

Copper is known for its corrosion resistance. It forms a green oxide layer that helps to protect it from further oxidation.

5.3.1 Potentiodynamic Tests

As shown in Figure 5-3 there was quite a bit of variability in the potentiodyanmic curves for the ten copper clad specimen tests. It can be seen that there are two clusters of values that are similar and they do not vary by much. Also shown is one test that is an outlier. This test will be ignored in analysis as it does not accurately represent what is happening. The active, passive and transpassive ranges are not well defined and seem to vary from one cluster of results to the next.

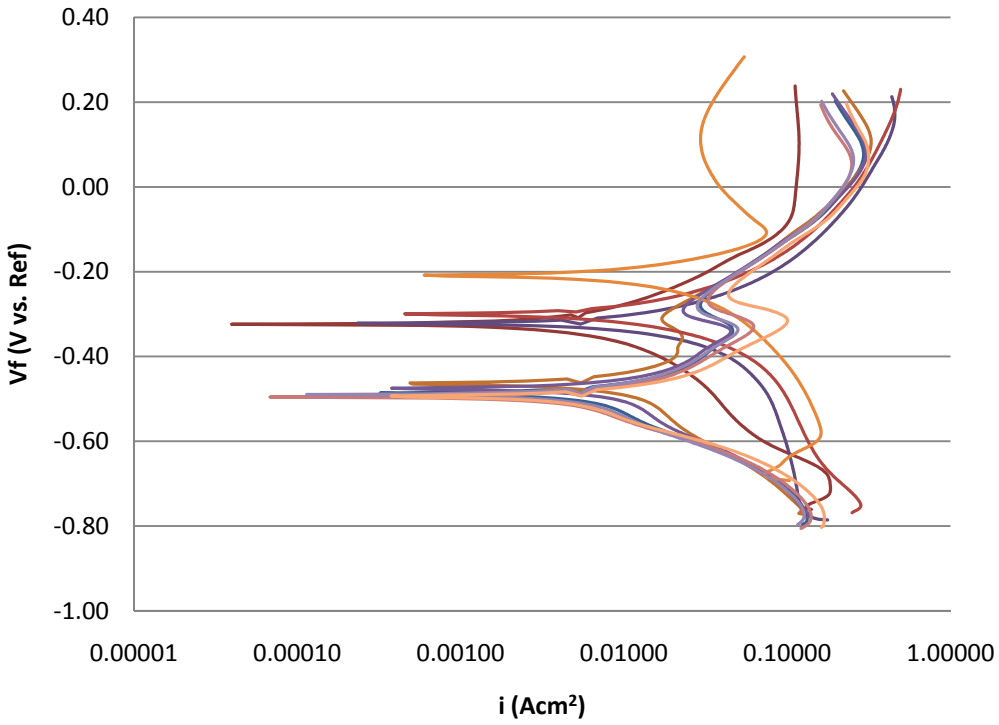

Figure 5-3: Potentiodynamic plot of copper clad strand tests

5.3.2 Linear Polarization Resistance Tests

As shown in Figure 5-3 and also in Figure 5-4 there is one test that does not match any of the other tests. This test will be ignored when calculating the averages. It can be seen in Figure 5-4 that once that single test is removed that there is not much variability between the other results. Thus an average of the other results will be used to represent the copper clad specimens.

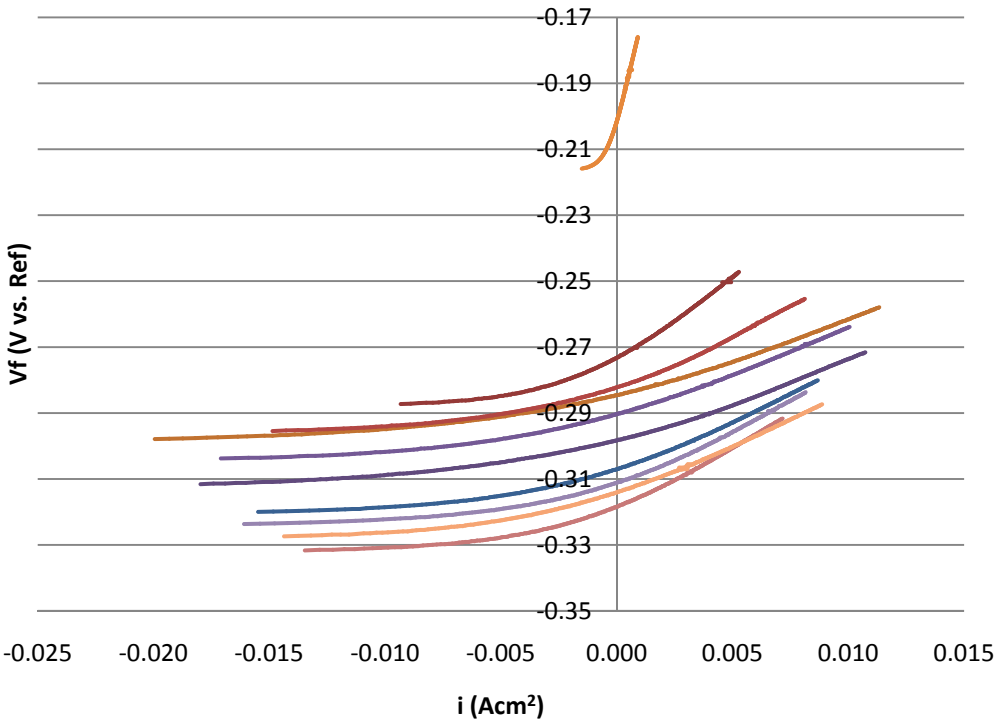

Figure 5-4: Linear polarization resistance plot of copper clad strand tests

The low variability is also shown in the values for the polarization resistance shown in Table 5-2. Excluding the outlying value (Test 7) the average polarization resistance, $R_{p\ AVG}$ = 11.68 kΩcm^2 and the average corrosion potential, $E_{corr\ AVG}$ = -298 mV_{SCE}.

Table 5-2: Linear polarization resistance results for copper clad strand tests

	Test 1	*Test 2*	*Test 3*	*Test 4*	*Test 5*	*Test 6*	*Test 7*	*Test 8*	*Test 9*	*Test 10*
Polarization Resistance, R_p ($k\Omega cm^2$)	11.18	18.97	8.502	8.290	11.21	9.925	119.9	13.97	11.56	11.50
Corrosion Potential, E_{corr} (mV vs. ref)	-307	-273	-298	-285	-282	-290	-202	-319	-311	-314

5.4 FLOW FILLED EPOXY COATED

In order for any results to be obtained from the flow filled epoxy coated strand specimens the epoxy coating was purposely damaged. The damage represented what damage would have been done by end grips when the strand is tensioned. This only allowed for a small area of the steel strand below the epoxy to be exposed to the grout. This can be held accountable for the high polarization resistance values obtained.

5.4.1 Potentiodynamic Tests

When the epoxy strands were purposely damaged it was done by gripping the ends and applying a force to sink the grips into the epoxy coating. Thus no two strands were damaged exactly the same. This could be blamed for the wide scatter in results shown in Figure 5-5. The active, passive and transpassive ranges seem to be very distinct however. All the plots follow the same trend also.

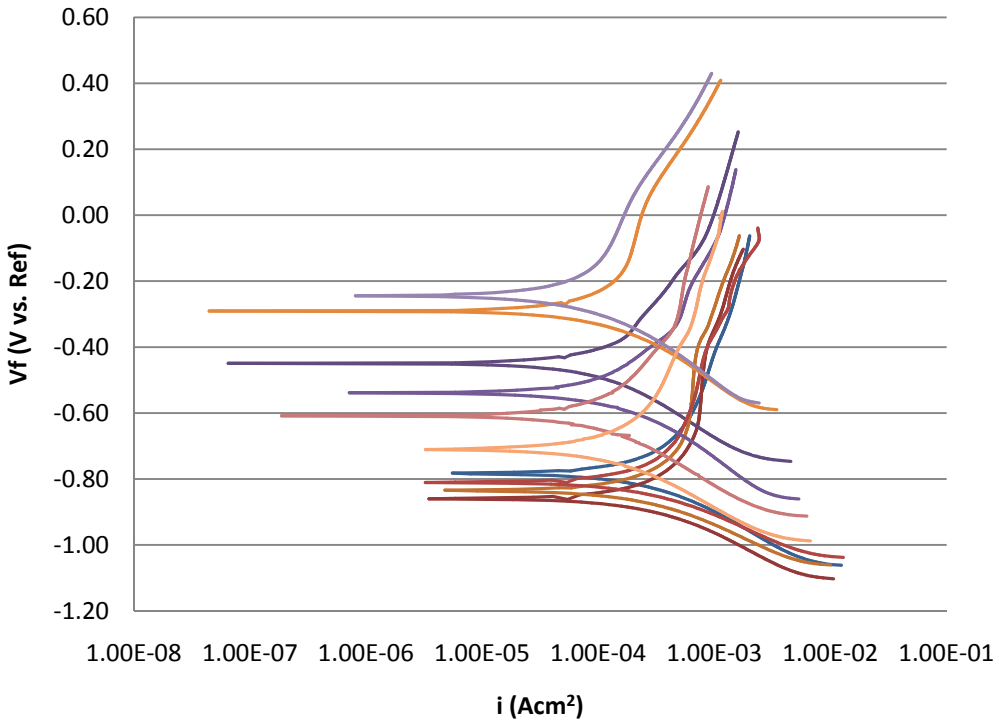

Figure 5-5: Potentiodynamic plot of flow filled epoxy coated strand tests

5.4.2 Linear Polarization Resistance Tests

The variability shown in Figure 5-5 is also reflected in Figure 5-6. The plot shows how variable the E_{corr} values were. However, there are not any distinct outliers and so all tests were considered in analysis.

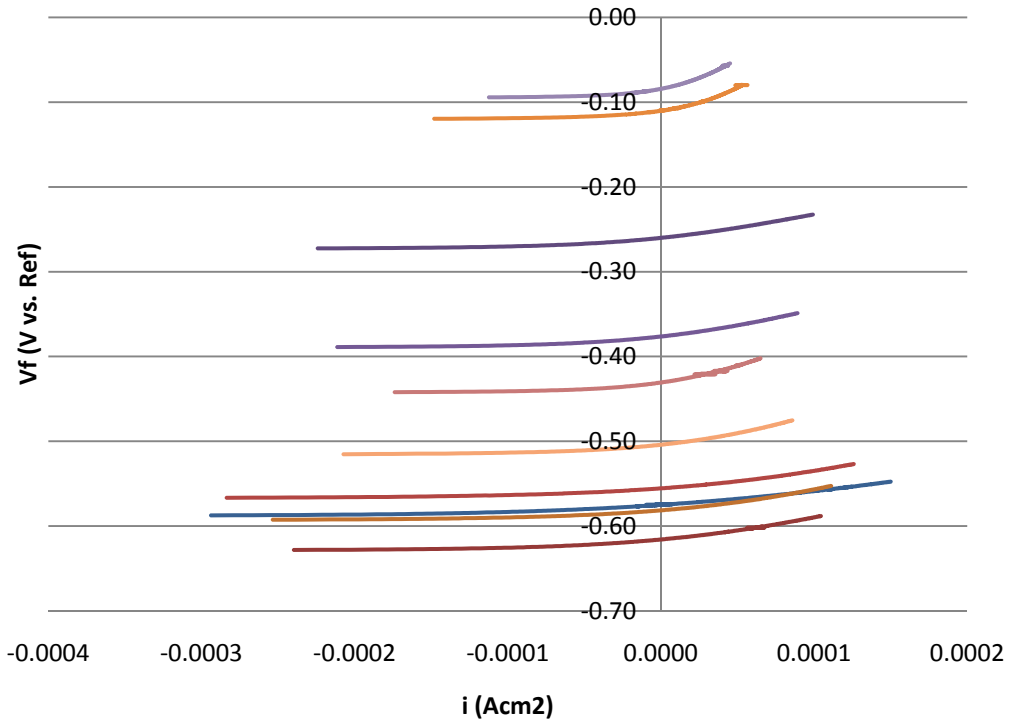

Figure 5-6: Linear polarization resistance plot of flow filled epoxy coated strand tests

Table 5-3 shows the calculated values for the polarization resistance and also the corrosion potential for the epoxy coated strand specimens. The variability in results can also be seen in this table. Considering all values the average polarization resistance, $R_{p\ AVG}$ = 1000 kΩcm^2 and the average corrosion potential, $E_{corr\ AVG}$ = -409 mV_{SCE}.

Table 5-3: Linear polarization resistance results for flow filled epoxy coated strand tests

	Test 1	*Test 2*	*Test 3*	*Test 4*	*Test 5*	*Test 6*	*Test 7*	*Test 8*	*Test 9*	*Test 10*
Polarization Resistance, R_p ($k\Omega cm^2$)	630.1	835.6	952.9	720.0	649.5	996.3	1262	1283	1708	961.4
Corrosion Potential, E_{corr} (mV vs. ref)	-575	-616	-260	-582	-556	-376	-110	-431	-84	-504

5.5 HOT DIP GALVANIZED

The hot dip galvanizing process involves immersing the strand in molten zinc to coat it. This process does not allow for a uniform coating of zinc to be applied. There can be a buildup of zinc in the crevices and interstitial areas of the strand. Variable thicknesses of the zinc coating can be blamed for the variability in the data. This is because the zinc coating is more active on the galvanic series than the steel strand which it is coating.

5.5.1 Potentiodynamic Tests

There are three clusters of results with one result sitting in between all the other results. As stated earlier the variable thickness of the zinc coating could be to blame for the scatter in the results. Most of the results only show an active range. This matches the properties of zinc. Zinc is used as a sacrificial anode in most marine applications so it only makes sense that the zinc coating would be in the active range for it to be sacrificed. The plots of all ten tests can be seen in Figure 5-7.

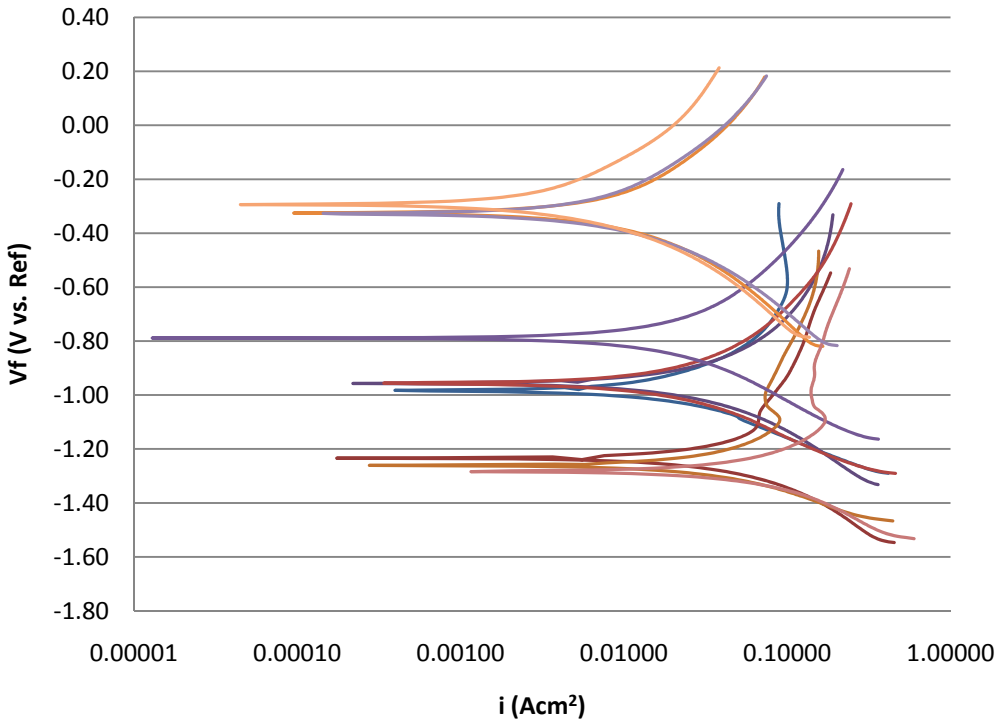

Figure 5-7: Potentiodynamic plot of hot dip galvanized strand tests

5.5.2 Linear Polarization Resistance Tests

Very similar to what was seen in Figure 5-7, Figure 5-8 shows a large scatter in the data. There are two clusters of data that sit on the two ends of the range. In between these two clusters are two tests that do not seem to correlate to the others.

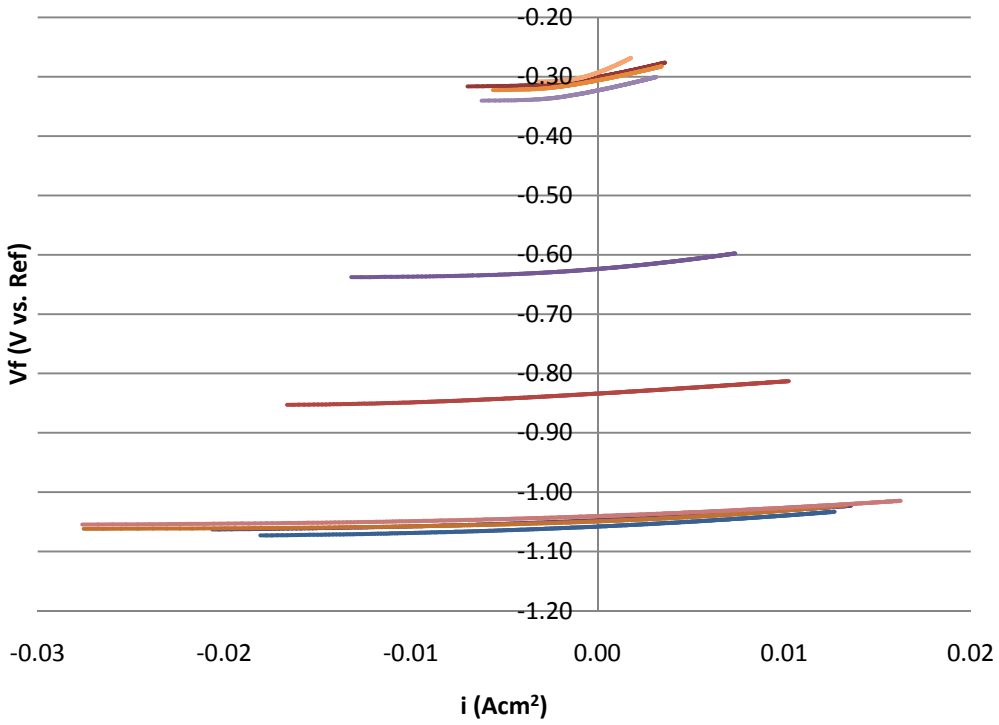

Figure 5-8: Linear polarization resistance plot of hot dip galvanized strand tests

Table 5-4 shows how variable the data is also. As the E_{corr} value gets more negative the R_p value goes down. Because there are two clusters of data and two other tests seem to sit right in the middle all the data was used in finding the averages. The average polarization resistance, $R_{p\ AVG}$ = 20.06 kΩcm^2 and the average corrosion potential, $E_{corr\ AVG}$ = -687 mV_{SCE}.

Table 5-4: Linear polarization resistance results for hot dip galvanized strand tests

	Test 1	*Test 2*	*Test 3*	*Test 4*	*Test 5*	*Test 6*	*Test 7*	*Test 8*	*Test 9*	*Test 10*
Polarization Resistance, R_p ($k\Omega cm^2$)	7.394	29.56	6.895	6.253	9.538	13.05	31.25	5.700	33.28	57.64
Corrosion Potential, E_{corr} (mV vs. ref)	-1058	-300	-1047	-1049	-834	-624	-306	-1040	-323	-293

5.6 STAINLESS CLAD

Stainless clad strands adapt the same concept as the copper clad strands. However, it uses the more expensive and corrosion resistant metal to clad conventional steel strand. The corrosion properties of the stainless steel strand should therefore be very similar to that of the solid stainless steel strand. There will be a slight difference however depending of the properties of the different stainless steels. Some stainless steels can be more corrosion resistant than others.

5.6.1 Potentiodynamic Tests

The plots of the stainless clad tests shown in Figure 5-9 have very little scatter. The scatter is similar to the scatter seen in the results of the conventional tests. Note the very distinct passive range seen in all the results also. In fact all the ranges, active, passive and transpassive are well defined. At the average corrosion potential of -201 mV_{SCE} all the tests show that the stainless steel strand is in its passive range.

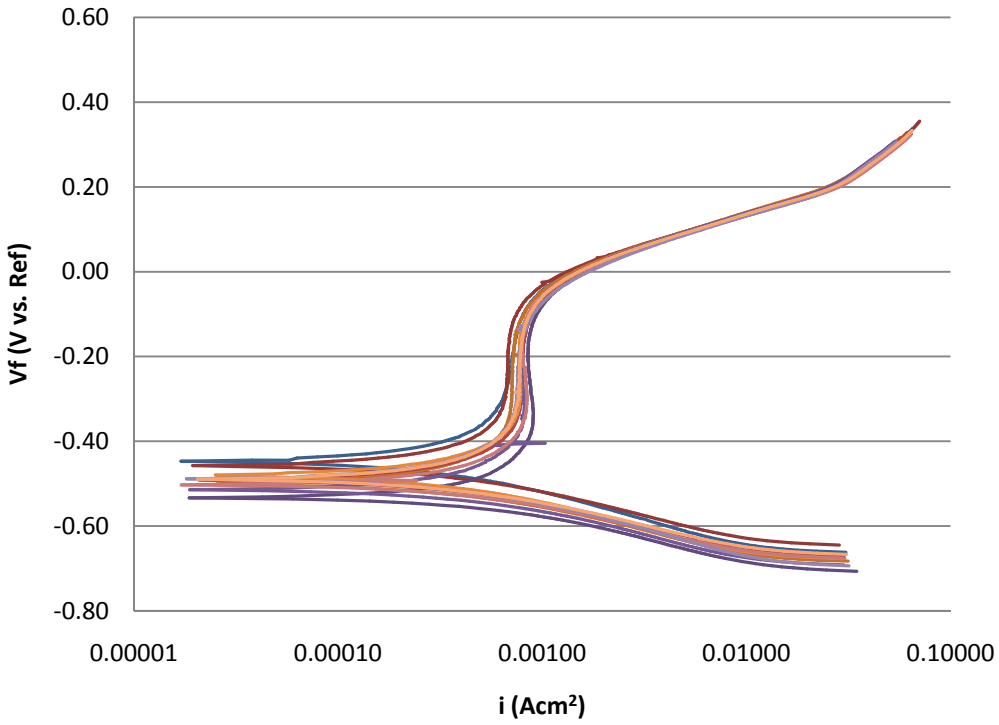

Figure 5-9: Potentiodynamic plot of stainless clad strand tests

5.6.2 Linear Polarization Resistance Tests

Figure 5-10 shows how similar the linear polarization resistance results were also. The slopes at E_{corr} are almost identical.

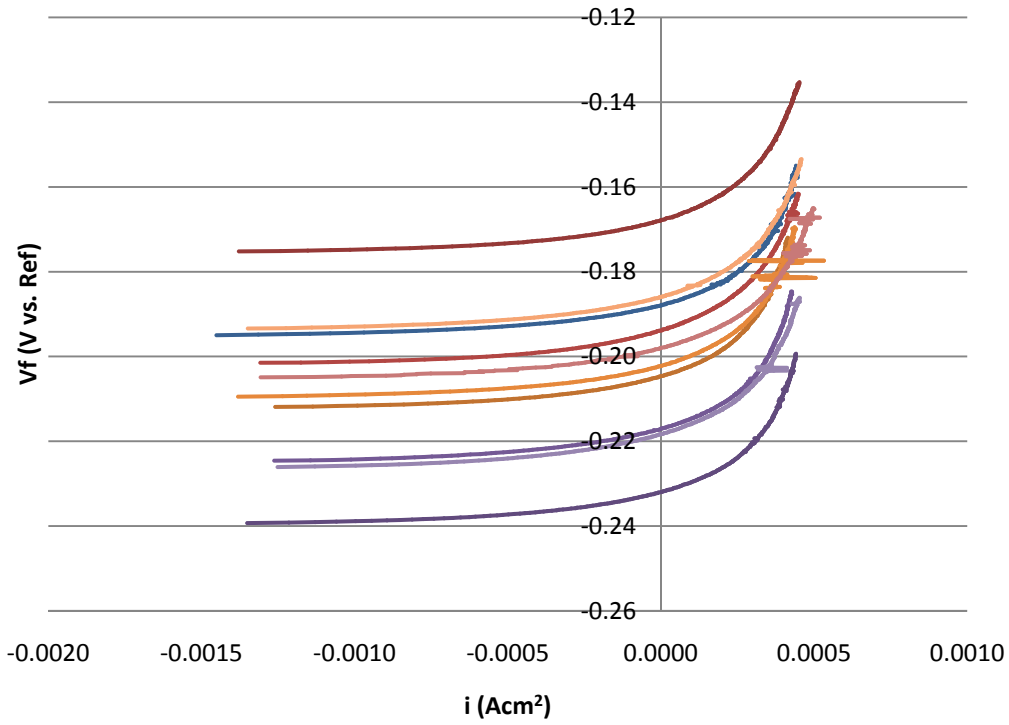

Figure 5-10: Linear polarization resistance plot of stainless clad strand tests

All the tests were used to find the average polarization resistance and the average corrosion potential. There was very little difference in the values obtained for the polarization resistance. The average polarization resistance, $R_{p\ AVG}$ = 92.72 $k\Omega cm^2$ and the average corrosion potential, $E_{corr\ AVG}$ = -201 mV_{SCE}.

Table 5-5: Linear polarization resistance results for stainless clad strand tests

	Test 1	*Test 2*	*Test 3*	*Test 4*	*Test 5*	*Test 6*	*Test 7*	*Test 8*	*Test 9*	*Test 10*
Polarization Resistance, R_p ($k\Omega cm^2$)	81.36	95.51	89.87	95.76	103.4	91.82	92.30	87.82	97.13	92.22
Corrosion Potential, E_{corr} (mV vs. ref)	-188	-168	-232	-205	-194	-217	-202	-198	-218	-186

5.7 STAINLESS STEEL

Stainless steel is known for its corrosion resistance and is often used in marine applications. The corrosion resistance of stainless steel depends on the grade which is used. And the grade depends on the percent of chromium used in the makeup of the metal. Chromium is the element that combined with other elements helps stainless steel to develop its stable oxide film[15]. This film protects the stainless steel from corrosive attack.

5.7.1 Potentiodynamic Tests

As expected the plots in Figure 5-11 clearly resemble the plots in Figure 5-9. There is more scatter in the results for the solid stainless steel strands however. There is still clearly defined active, passive and transpassive ranges however. At the average corrosion potential of -243 mV_{SCE} it appears that all the stainless steel strands were in the passive state.

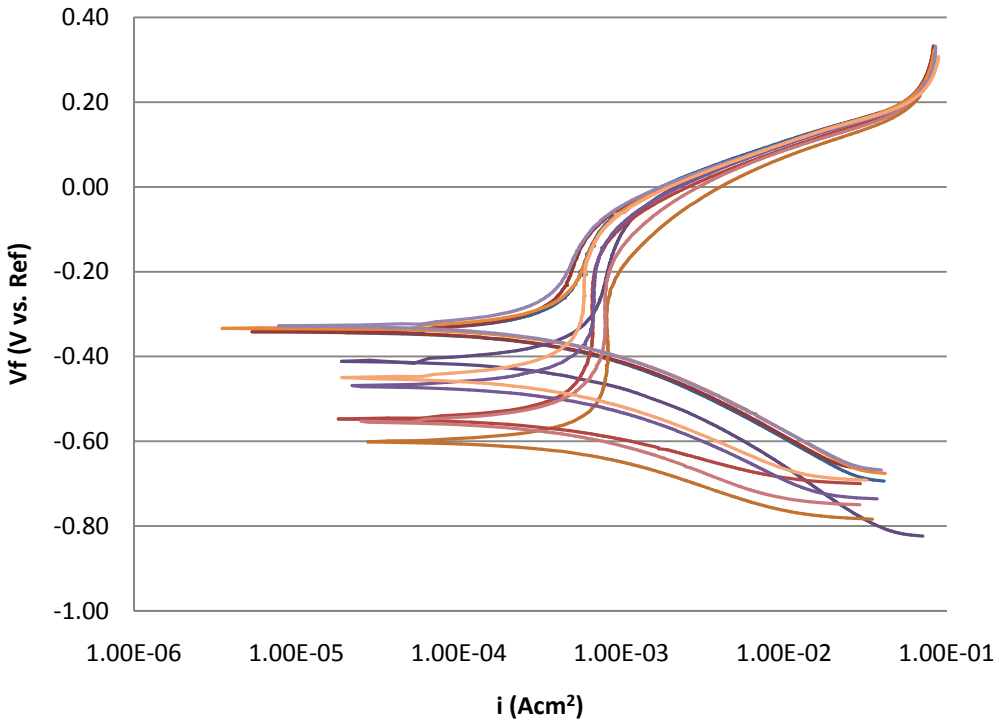

Figure 5-11: Potentiodynamic plot of stainless steel strand tests

5.7.2 Linear Polarization Resistance Tests

The scatter in Figure 5-11 is reflected in Figure 5-12. There does seem to be a cluster of values at the higher potentials however. Also there does not seem to be any outlying values and thus no values will be ignored in calculating the averages.

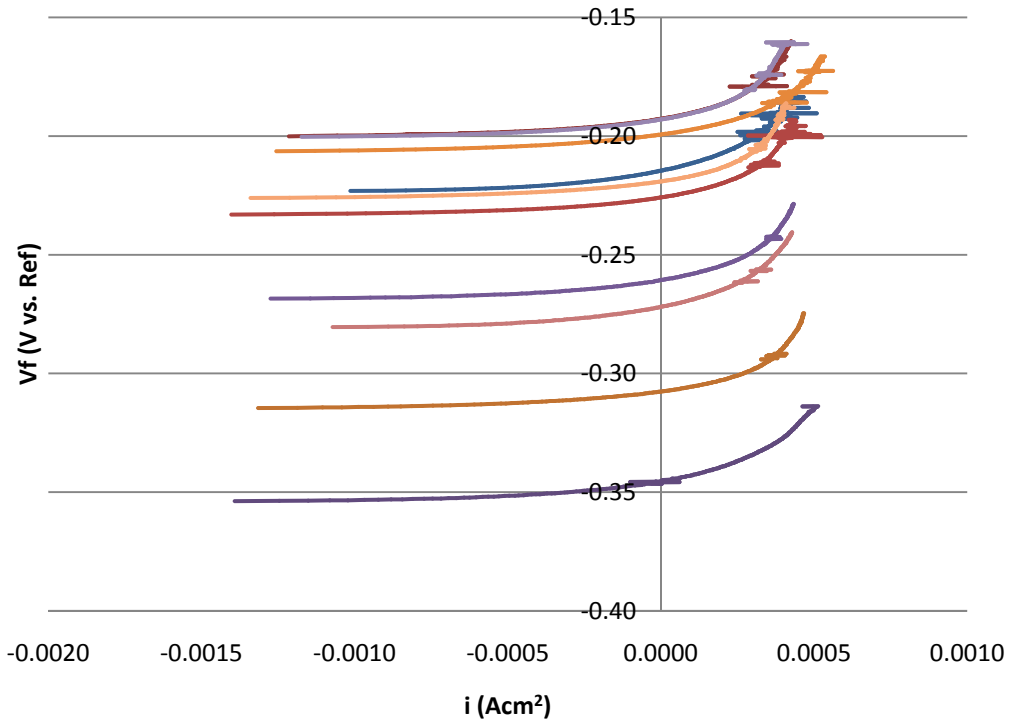

Figure 5-12: Linear polarization resistance plot of stainless steel strand tests

Using all the values in Table 5-6 the average polarization resistance, $R_{p\ AVG}$ = 100.5 kΩcm^2 and the average corrosion potential, $E_{corr\ AVG}$ = -243 mV_{SCE}.

Table 5-6: Linear polarization resistance results for stainless steel strand tests

	Test 1	*Test 2*	*Test 3*	*Test 4*	*Test 5*	*Test 6*	*Test 7*	*Test 8*	*Test 9*	*Test 10*
Polarization Resistance, R_p (kΩcm^2)	129.7	96.91	110.6	77.19	92.99	105.3	82.77	124.9	99.88	84.42
Corrosion Potential, E_{corr} (mV vs. ref)	-215	-193	-345	-308	-226	-261	-199	-272	-193	-219

5.8 SUMMARY

The conventional strand was used as a base value for comparison of the other strand types. Therefore all the values were standardized versus the conventional value. A summary of the linear polarization resistance results is shown in Table 5-7.

Table 5-7: Summary of the linear polarization resistance results for all tests

	Conventional	*Copper Clad*	*Flow Filled Epoxy Coated*	*Hot Dip Galvanized*	*Stainless Clad*	*Stainless Steel*
Avg Polarization Resistance, $R_{p\ AVG}$ ($k\Omega cm^2$)	10.82	11.68	1000	20.06	92.72	100.5
Vs. Conventional	1.00	1.08	92.4	1.85	8.57	9.28
Avg Corrosion Potential, $E_{corr\ AVG}$ (mV vs. ref)	-601	-298	-409	-687	-201	-243

As stated in Chapter 4, Dr. Pacheco and Dr. Schokker found a relation between the polarization resistance and the time to corrosion[18]. Using this basis, the polarization resistance values calculated from the tests were used to compare the times to corrosion for the different strand types. The relation is a linear relation where $t_{corr} = 1.25\ R_p$, where t_{corr} is in hours and R_p is in $k\Omega cm^2$. In the PTI ballot proposal[24] however, it states that the R_p of the grout being tested should be no less than 700 $k\Omega cm^2$. An area of 291 cm^2 was used in their testing compared with 71.8 cm^2 used in these tests. Even if the area of 291 cm^2 is used to compare the different tests, the results obtained from this testing does not match the results obtained by Dr. Pacheco and Dr. Schokker. Thus the relation where $t_{corr} = 1.25\ R_p$ did not apply to this testing. The concept that the time to corrosion and the polarization resistance values are related to each other was adapted to this testing

however. Since it is only a comparison between the different strand types it was not important to establish set values for the time to corrosion for each strand type.

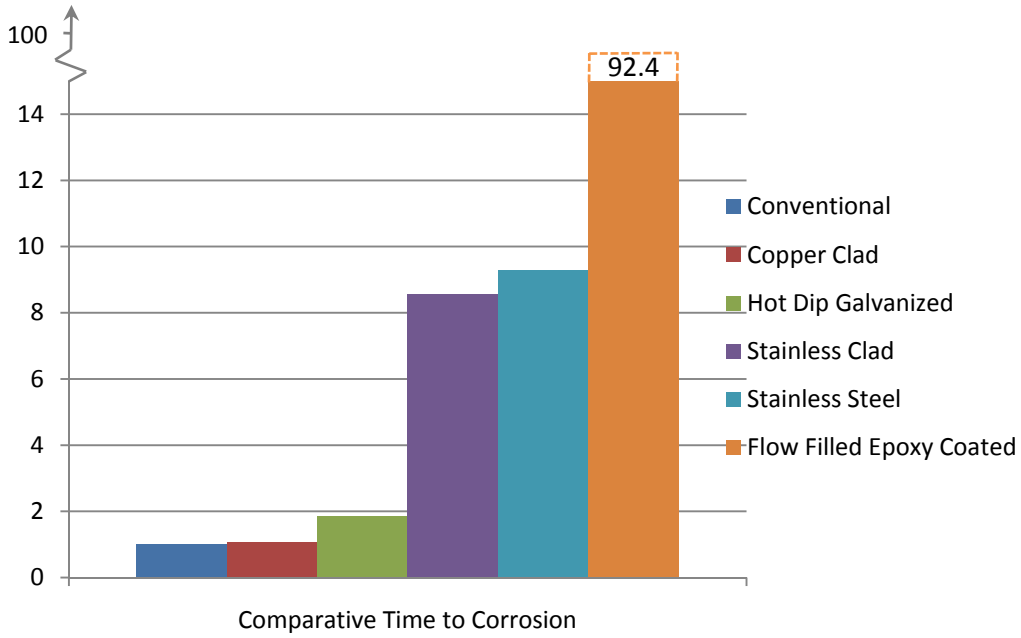

Figure 5-13: Bar chart showing comparison of times to corrosion

The time to corrosion is not known for the conventional strand so a time to corrosion value cannot be listed for each strand type. They can only be compared side by side with the other strand types. From the results shown in Figure 5-13 it is clear that all the strand types tested performed better than the conventional base strand. The y-axis maximum value was capped at 15 to better show the comparison between all the strand types. The full flow filled epoxy coated bar on the chart is therefore not shown. The copper cladding does not help very much in prolonging the time till corrosion initiates. The hot dip galvanizing process delays the onset of corrosion but still not by much. It appears to be twice as long as conventional. The stainless clad and solid stainless steel performed very similar

which was expected. Both taking about 9 times as long as conventional strand for corrosion to initiate. The flow filled epoxy coated result is a lot larger than all the other results. The smaller area that was exposed to the grout is the major factor. This result only applies to ends where the strand is gripped and also where there are tears in the epoxy coating. If the epoxy coating is not damaged there would be no possibility for corrosion initiating.

CHAPTER 6
Conclusions and Recommendations

6.1 CONCLUSIONS

6.1.1 Mechanical Testing

The mechanical tests were used to determine how well the prestressing strands met the requirements for use in service. From the origins of the project it was recognized that the copper clad strands were not ½ in. diameter structural strands. Their unclad diameter and properties were basically that of 0.438 in. diameter strand. They were included in the testing primarily for their corrosion resistance. So it was expected that they would not meet the ½ in. strand requirements for use in industry. If the corrosion resistance was highly superior, it was planned to try copper cladding of higher strength strand in a later phase. All the other strand types tested have been or were expected to be used in the field. The calculated properties of each strand type are shown in Table 6-1.

Table 6-1: Summary of the mechanical tests including modulus info

Type	*Nominal Dia. (in)*	*Breaking Strength (kip)*	*Yield Strength (kip)*	*Elastic Modulus (ksi)*	*Secant Modulus (ksi)*
Conventional	0.6	61.5	56.1	29396	29378
Conventional	0.5	43.0	37.3	28664	28609
Epoxy Coated	0.5	43.7	37.8	29249	29046
Stainless Clad (nominal area)	0.6	57.5	50.6	27148	26725
Stainless Clad (steel area)	0.6	57.5	50.6	38505	37904
Hot Dip Galvanized	0.5	40.9	34.5	28846	28830
Stainless Steel	0.6	48.9	39.8	-	21116
Copper Clad (nominal area)	0.5	25.9	22.3	-	22024
Copper Clad (steel area)	0.5	25.9	22.3	-	29365

The breaking strength and the yield strength of each strand type were compared to the requirements set in ASTM 416. A bar chart showing the ultimate strengths of the different strand types is shown in Figure 6-1. The required breaking strengths for each diameter and grade are shown on the bar chart. Using these requirements it is possible to see what strands met what requirements.

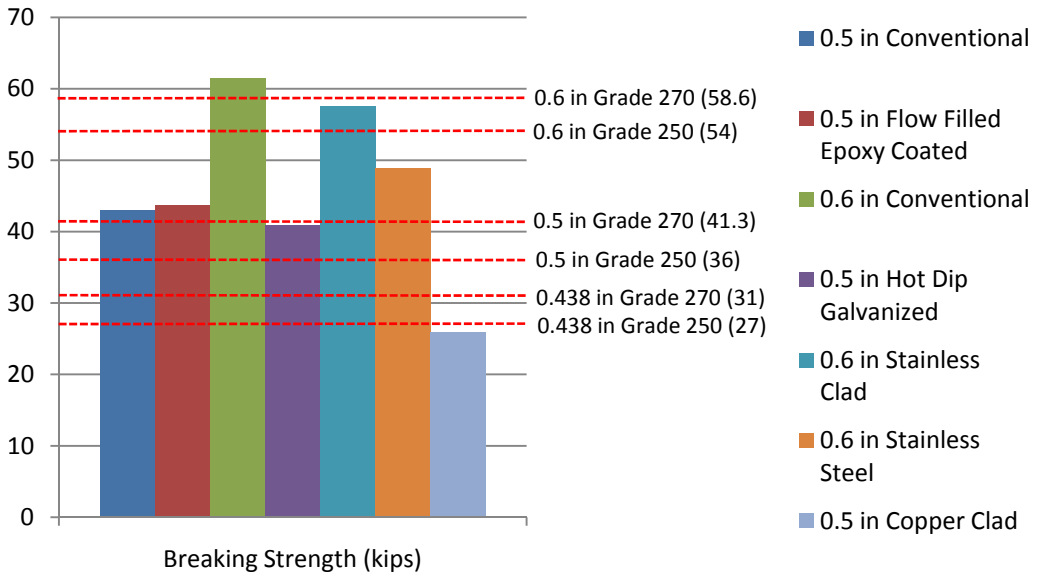

Figure 6-1: Bar chart showing breaking strengths

The 0.6 in. conventional strand met the 0.6 in. Grade 270 requirement. However the stainless clad and the stainless steel strands did not meet this Grade 270 requirement. The stainless clad did however meet the Grade 250 requirement. All of the 0.5 in. strands met or came close to meeting the Grade 270 requirement for 0.5 in. strands. The hot dip galvanized strand came close to meeting the requirement but did not because it lost some of its strength due to the heat in the galvanizing process. If the cladding on the copper clad strand is considered structural and part of the area then the copper clad strand did not meet the requirements for 0.5 in. strand. If the cladding is not considered structural and the strand is considered to be 0.438 in. in diameter which is the diameter of the steel core then the strand still does not meet the requirements.

The yield strengths of the strands are shown in Figure 6-2 and Figure 6-3. Figure 6-2 compares the strands to the yield strength requirements for low-

relaxation strand. Figure 6-3 compares the strands to the yield strength requirements for normal-relaxation strand.

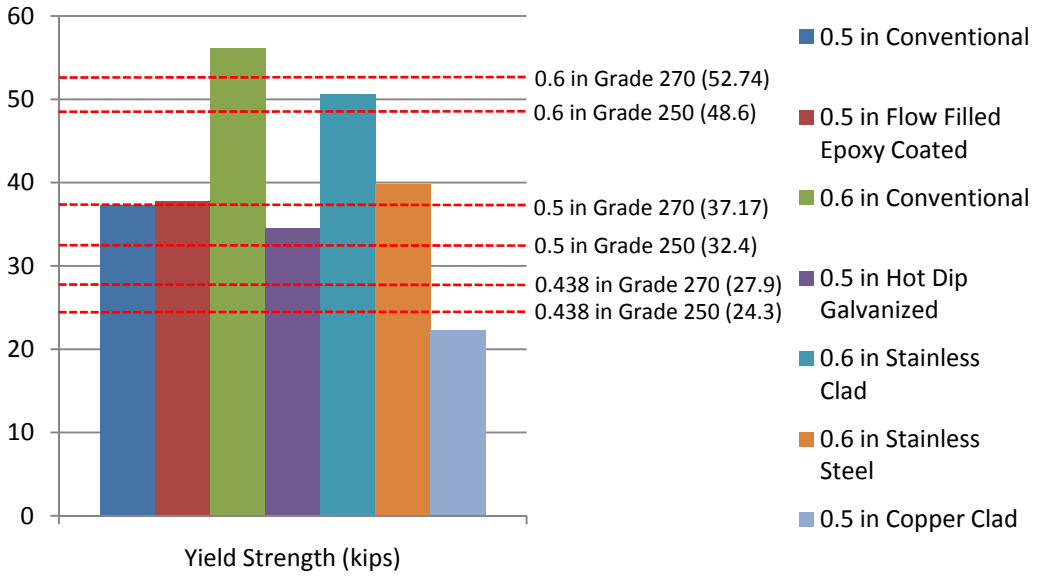

Figure 6-2: Bar chart showing yield strengths (compared to low-relaxation)

The 0.6 in. conventional strand clearly meets the yield strength requirements for 0.6 in. Grade 270 low-relaxation strand. The stainless clad does not meet the Grade 270 requirement but meets the Grade 250 requirement. Once again the stainless steel strand did not meet any of the 0.6 in. requirements. The 0.5 in. conventional and the flow filled epoxy strands met the Grade 270 yield strength requirement for 0.5 in. strands. The hot dip galvanized strand only met the Grade 250 requirement for 0.5 in. strand. This can again be blamed on a loss of strength in the galvanizing process. The copper clad strand did not meet the requirements for either the 0.438 in. diameter strand or the requirements for 0.5 in. diameter strand.

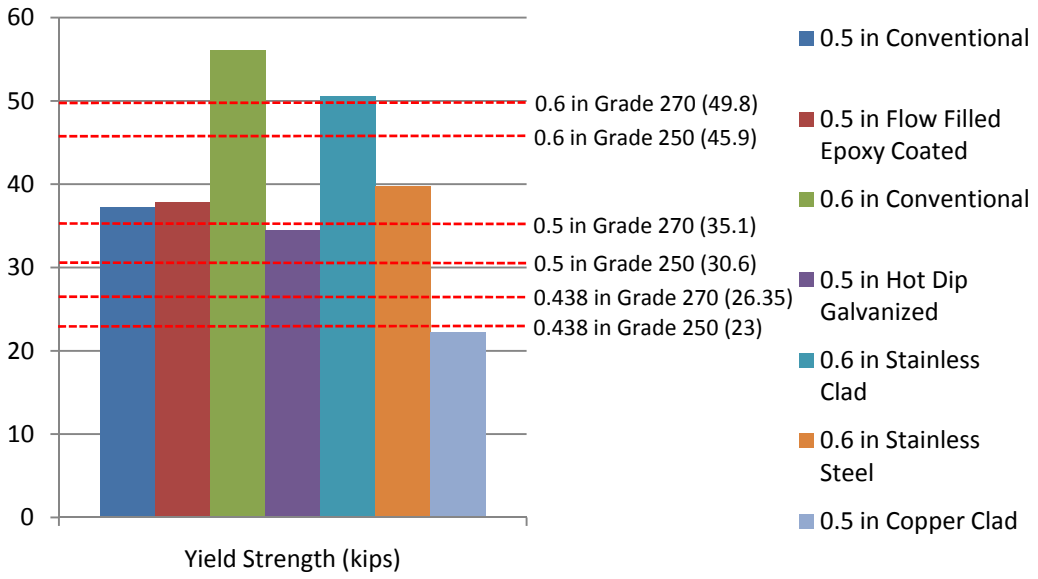

Figure 6-3: Bar chart showing yield strengths (compared to normal-relaxation)

The normal-relaxation requirements are lower than the low-relaxation requirements. The results when compared to the normal-relaxation values are very similar to that when compared to the low-relaxation values. The only significant difference is that the stainless clad strand meets the 0.6 in Grade 270 requirements for normal-relaxation strand whereas it does not meet it for low-relaxation.

As expected the copper clad strands did not meet the requirements for 0.5 in. strands. They did not meet the requirements for 0.438 in. diameter strands either. In order for a strand of this type to be considered for use in the field more research must be done. The solid stainless steel strand tested was originally destined for use in a bridge project in California. However the mechanical tests show that this stainless steel strand does not meet the required strengths. Also notable is the fact that both the stainless steel strand and the copper clad strands

did not have a well defined elastic region and thus an elastic modulus could not be determined for either strand type. The secant modulus was provided for comparison of all strand types.

All the other strand types had very similar stress vs. strain behaviors. The two strand types with slightly lower yield and ultimate strengths were the stainless clad and the galvanized coated. This was expected. The stainless cladding on the stainless clad strand helps to protect the strand from corrosion. However it reduces the overall strength of the strand because stainless steel is naturally not as strong as conventional steel. The galvanized strand becomes weaker during the galvanizing process. The heat that the steel is exposed to in the galvanizing process weakens it and this can be seen in the stress vs. strain plot shown in Figure 6-4.

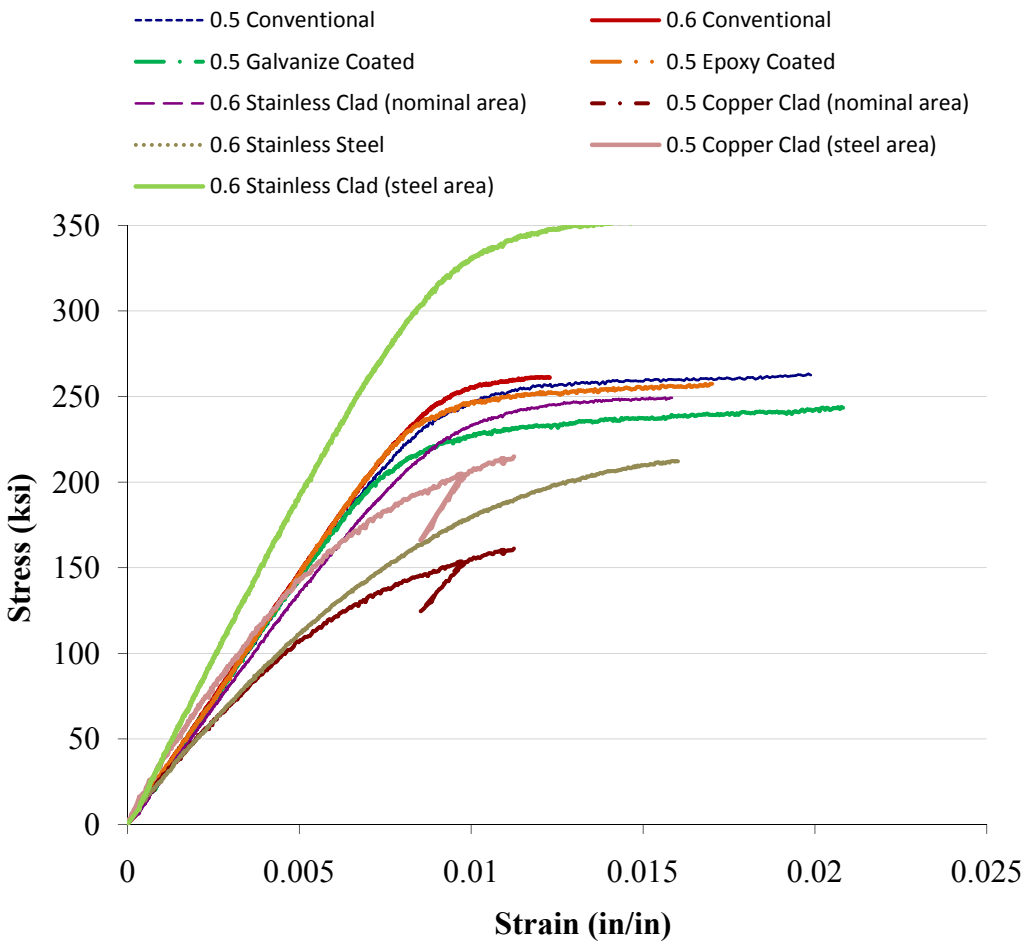

Figure 6-4: Stress vs. Strain plot of all strand types

6.1.2 Accelerated Corrosion Testing

Originally it was thought that the standard potentiostatic accelerated corrosion test would be an acceptable test method for comparison of the strand types. However after preliminary potentiodynamic tests were performed on each strand type the potentiostatic test was abandoned. The results of the potentiodynamic tests showed that it was not possible to choose a single potential to run the potentiostatic tests. Using Dr. Andrea Schokker's PTI ballot proposal as

a basis, the linear polarization resistance test was used instead. A summary of the linear polarization test results is shown in Table 6-2.

Table 6-2: Summary of the linear polarization resistance results for all tests

	Conventional	*Copper Clad*	*Flow Filled Epoxy Coated*	*Hot Dip Galvanized*	*Stainless Clad*	*Stainless Steel*
Avg Polarization Resistance, $R_{p\ AVG}$ ($k\Omega cm^2$)	10.82	11.68	1000	20.06	92.72	100.5
Vs. Conventional	1.00	1.08	92.4	1.85	8.57	9.28
Avg Corrosion Potential, $E_{corr\ AVG}$ (mV vs. ref)	-601	-298	-409	-687	-201	-243

Dr. Pacheco and Dr. Schokker found a relation between the polarization resistance and the time to corrosion[18]. This relation is explained in detail in earlier chapters. The exact relation was not used in this comparison however. Only the basis of the relation was used for comparison. Since the strands were only to be compared side by side it was not important for a specific time to corrosion to be established for each strand type. Therefore the results shown are primarily for comparison and do not suggest time to corrosion values for the strands.

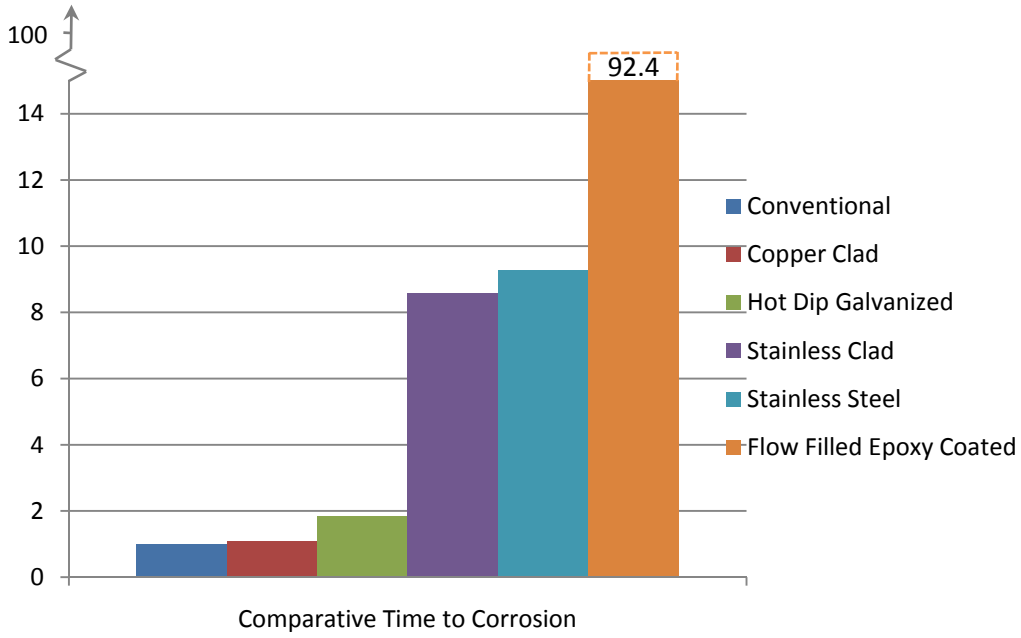

Figure 6-5: Bar chart showing comparison of times to corrosion

The conventional strand was used as a base for the comparison of the times to corrosion for the strand types. It can be seen in Figure 6-5 that all of the strand types performed better than the conventional strand. The copper cladding, although helping to increase the corrosion resistance of the strand did not change the time to corrosion by very much. The hot dip galvanizing process reduced the strength of the strand by approximately 5% but increased the time to corrosion by nearly double that of conventional strand. The stainless steel strand and also the stainless clad strand had similar results. They both showed that stainless steel increases the time to corrosion of the strand. Both increased the time to corrosion by approximately 9 times that of conventional strand. The flow filled epoxy coated results are quite high due to the fact that the area exposed to grout is a lot less than all the other specimens. It is difficult to compare the flow filled epoxy

coated strand side by side with the other strands because of this disparity in the area in contact with the grout. However if the epoxy coating is not damaged there should not be any type of corrosion forming on the strand because the epoxy coating fully protects the conventional strand below. So the higher time to corrosion for the flow filled epoxy coated strand is quite realistic.

6.2 RECOMMENDATIONS

At this point it appears that the stainless clad and the flow filled epoxy coated strands have performed the best. As stated earlier if the epoxy coating is not damaged it will provide long lasting corrosion resistance. The ends where the strands are anchored must be protected so that corrosion cannot start at the anchorages. The stainless clad strands have slightly less strength than the conventional strands but they still meet the strength requirements. The stainless cladding also helps to increase the time to corrosion by approximately 9 times that of conventional strand. The ends that are cut must also be protected to prevent corrosion of the conventional steel below the stainless cladding.

The solid stainless steel and the copper clad strands did not meet the strength requirements and should not be used in service. More research needs to be done to develop stainless steel and copper clad strands that meet the strength requirements.

6.3 RECOMMENDATIONS FOR FUTURE TESTING

The corrosion testing done in this thesis was based on a test method used to compare grouts. Therefore more testing needs to be done to guarantee the accuracy of the test method used to compare the different strand types. Long term exposures to salt solution may be the best method to assure the accuracy of the results.

Testing of the strands after the salt solution has penetrated through to the grout/strand surface also should be performed. This testing will give an idea of the corrosion rate of the strands once the salt solution has gotten through the grout protective surface. Pre-cracking the grout and using the linear polarization resistance test method may produce acceptable results.

BIBLIOGRAPHY

1. Ahern, M.E. (2005). *Design and Fabrication of a Compact Specimen for Evaluation of Corrosion Resistance of New Post-Tensioning Systems*. MSc. Thesis, The University of Texas at Austin.

2. ASTM A 370 (2005). Standard Test Methods and Definitions for Mechanical Testing of Steel Products. *American Society for Testing and Materials*, West Conshohocken, PA.

3. ASTM A 416/A 416M (2006). Standard Specification for Steel Strand, Uncoated Seven-Wire for Prestressed Concrete. *American Society for Testing and Materials*, West Conshohocken, PA.

4. ASTM A 931 (2002). Standard Test Method for Tension Testing of Wire Ropes and Strand. *American Society for Testing and Materials*, West Conshohocken, PA.

5. ASTM C 876 (1999). Standard Test Method for Half-Cell Potentials of Uncoated Reinforcing Steel in Concrete. *American Society of Testing and Materials*, West Conshohocken, PA.

6. ASTM G 1 (2003). Standard Practice for Preparing, Cleaning, and Evaluating Corrosion Test Specimens. *American Society of Testing and Materials*, West Conshohocken, PA.

7. ASTM G 102 (2004). Standard Practice for Calculation of Corrosion Rates and Related Information from Electrochemical Measurements. *American Society of Testing and Materials*, West Conshohocken, PA.

8. ASTM G 15 (2007). Standard Terminology Relating to Corrosion and Corrosion Testing. *American Society of Testing and Materials*, West Conshohocken, PA.

9. ASTM G 3 (2004). Standard Practice for Conventions Applicable to Electrochemical Measurements in Corrosion Testing. *American Society of Testing and Materials*, West Conshohocken, PA.

10. ASTM G 5 (2004). Standard Reference Test Method for Making Potentiostatic and Potentiodynamic Anodic Polarization Measurements. *American Society of Testing and Materials*, West Conshohocken, PA.

11. ASTM G 59 (2003). Standard Test Method for Conducting Potentiodynamic Polarization Resistance Measurements. *American Society of Testing and Materials*, West Conshohocken, PA.

12. Hamilton, H.R. (1995). *Investigation of Corrosion Protection Systems for Bridge Stay Cables*. PhD Dissertation, The University of Texas at Austin.

13. Hansen, B. (2007). Tendon Failure Raises Questions about Grout in Posttensioned Bridges. *Civil Engineering News. 77(11)*, 17-18.

14. Hill, A.T. Jr. (2006). *Material Properties of the Grade 300 and Grade 270 Prestressing Strands and Their Impact on the Design of Bridges*. MSc. Thesis, Virginia Polytechnic Institute and State University.

15. Jones, D.A. (1996). *Principles and Prevention of Corrosion*. Prentice Hall (Second Edition)

16. Koester, B.D. (1995). *Evaluation of Cement Grouts for Strand Protection using Accelerated Corrosion Tests*. MSc. Thesis, The University of Texas at Austin.

17. Kouril, M., Novak, P., and Bojko, M. (2006). Limitations of the Linear Polarization Method to Determine Stainless Steel Corrosion Rate in Concrete Environment. *Cement and Concrete Composites, 28*, 228-225.

18. Pacheco, A.R. (2003). *Evaluating The Corrosion Protection of Post-Tensioning Grouts: Standardization of an Accelerated Corrosion Test*. PhD Dissertation, The Pennsylvania State University.

19. Pacheco, A.R., Schokker, A.J., and Hamilton, H.R. (2006). *Development of a Standard Accelerated Corrosion Test for Acceptance of Post-Tensioning Grouts in Florida*. University of Florida.

20. Preston, H.K. (1985). Testing 7-Wire Strand for Prestressed Concrete – The State of the Art, *PCI Journal*, 30(3), 134-155.

21. Reina, P. (2007). British Engineers Tackle Corroded Cables on Trio. *Engineering News Record*. *258(14)*, 14.

22. Salas, R.M., Schokker, A.J., West, J.S., Breen, J.E., and Kreger, M.E. (2004). *Project Summary Report 0-1405-S, Durability Design of Post-Tensioned Bridge Substructure Elements*. Center for Transportation Research, The University of Texas at Austin.

23. Schokker, A.J. (1999). *Improving Corrosion Resistance of Post Tensioned Substructures Emphasizing High Performance Grouts*. PhD Dissertation, The University of Texas at Austin.

24. Schokker, A.J. (2007). *Modifications to the PTI Specification for Grouting of Post-Tensioned Structures.* PTI Ballot Proposal.

25. Shenoy, C.V., and Frantz, G.D. (1991). A Simple Method of Gripping Prestressing Strands for Tension Tests. *PCI Journal*, 36(4), 58-65.

26. Thompson, N.G., Lankard, D., and Sprinkel, M. (1992). *Improved Grouts for Bonded Tendons in Post-Tensioned Bridge Structures*. Report No. FHWA-RD-91-092, Federal Highway Administration, Cortest Columbus Technologies.

27. Turco, G.P. (2007). *Durability Evaluation of Post-Tensioned Concrete Beam Specimens After Long-Term Aggressive Exposure Testing*. MSc. Thesis, The University of Texas at Austin.